

Neutralino pair production at CERN LHC[†].

G.J. Gounaris^a, J. Layssac^b, P.I. Porfyriadis^a and F.M. Renard^b

^aDepartment of Theoretical Physics, Aristotle University of Thessaloniki,
Gr-54124, Thessaloniki, Greece.

^bPhysique Mathématique et Théorique, UMR 5825
Université Montpellier II, F-34095 Montpellier Cedex 5.

Abstract

We consider the production of neutralino pairs $\tilde{\chi}_i^0 \tilde{\chi}_j^0$ at a high energy hadron collider, putting a special emphasis on the case where one of them is the lightest neutralino $\tilde{\chi}_1^0$, possibly constituting the main Dark Matter component. At tree level, the only relevant subprocess is $q\bar{q} \rightarrow \tilde{\chi}_i^0 \tilde{\chi}_j^0$, while the subprocess $gg \rightarrow \tilde{\chi}_i^0 \tilde{\chi}_j^0$ first appears at the one loop level. Explicit expressions for the $q\bar{q}$ -helicity amplitudes are presented, including the tree level contributions and the leading-log one loop radiative corrections. For the one-loop $gg \rightarrow \tilde{\chi}_i^0 \tilde{\chi}_j^0$ process, a numerical code named PLATONggn is released, allowing the computation of $d\sigma/d\hat{t}$ in any MSSM model with real soft breaking parameters. It turns out that acceptable MSSM benchmark models exist for which the $q\bar{q}$ and the gluonic contributions may give comparable effects at LHC, due to the enhanced gluonic structure functions at low fractional momenta. Depending on the values of the MSSM parameters, we find that the LHC neutralino pair production may provide sensitive tests of SUSY models generating neutralino Dark Matter.

PACS numbers: 12.15.-y, 12.15.Lk, 13.75.Cs, 14.80.Ly

[†]Work supported by the European Union under contract HPRN-CT-2000-00149.

1 Introduction

Neutralino production at hadron colliders is an important part of the program of Supersymmetry (SUSY) searches [1, 2]. One special reason is related to the possibility that $\tilde{\chi}_1^0$, the lightest neutralino state, is in fact the Lightest Supersymmetric Particle (LSP) [3]. This has two particular consequences; the first concerning the supersymmetric spectroscopy (chains and rates of decays) in R-parity conserving models [1]; while the second largely determining the search for Dark Matter (DM) [4].

DM detection in such a case is expected to occur either in a direct way (*e.g.* through the observation of nucleus recoil in $\tilde{\chi}_1^0 N \rightarrow \tilde{\chi}_1^0 N$ elastic scattering); or in an indirect way, by observing modifications of the cosmic spectrum of particles like photons, positrons, antiprotons etc., due to contributions from $\tilde{\chi}_1^0 \tilde{\chi}_1^0$ annihilation [5]. Concerning the indirect way, we have presented in two previous papers the results of a complete one-loop computation for the processes $\tilde{\chi}_i^0 \tilde{\chi}_j^0 \rightarrow \gamma\gamma, gg$ involved in DM annihilation [6], as well as the results for the reversed process of neutralino pair production at a photon-photon collider [7]. In [6] we have also emphasized that in certain benchmark MSSM models the gluon-gluon channel may be important for determining the neutralino relic density [8, 9, 10].

We would expect therefore, that for neutralino pair production at a high energy hadron collider like LHC, kinematical domains may exist where the gluon structure function of the proton is so large [11], that the one-loop gluon annihilation contribution may in fact be bigger than the tree level $q\bar{q}$ contribution. The precise study of such neutralino-pair production process at LHC, through the subprocesses $q\bar{q} \rightarrow \tilde{\chi}_i^0 \tilde{\chi}_j^0$ and $gg \rightarrow \tilde{\chi}_i^0 \tilde{\chi}_j^0$, constitutes the aim of the present paper.

First, we present the helicity amplitudes and cross sections of the subprocess $q\bar{q} \rightarrow \tilde{\chi}_i^0 \tilde{\chi}_j^0$ at tree level. At this level, such a process has been studied long ago *e.g.* in [12, 13]. We go beyond this though by also exploring the Fermi statistics and CP (for real MSSM parameters) constraints on these amplitudes, which strongly reduce their number and also serve as a check of the calculations.

In a second step, and in order to check the possible existence of important one-loop electroweak (EW) contributions to these $q\bar{q}$ amplitudes, the leading ($\alpha \ln^2 s$) and sub-leading ($\alpha \ln s$) contributions are included, following the procedure established in [14, 15, 16]. These EW corrections reduce the overall tree level magnitude of the amplitudes by an amount that can reach the few tens of percent level for the kinematical domain attainable at LHC. In the same direction acts also the SUSY QCD contribution¹ calculated according to the rules established to order $\alpha_s \ln s$ in [16, 17]. We should emphasize at this point though, that these EW and SUSY QCD corrections should be considered in addition to the pure QCD (leading and next-to-leading) corrections which strongly increase the tree level amplitudes, as found in [17].

We then turn to the one-loop subprocess $gg \rightarrow \tilde{\chi}_i^0 \tilde{\chi}_j^0$, for which the helicity amplitudes are calculated using the set of diagrams established in [6, 7]. There, the neutralino annihilation amplitudes $\tilde{\chi}_i^0 \tilde{\chi}_j^0 \rightarrow gg$ were calculated under any kinematical conditions;

¹These involve QCD interactions explicitly affecting SUSY particle exchanges [16].

but the accompanying numerical codes compute the neutralino MSSM annihilation cross section to gluons only at the appropriate for dark matter threshold region [18]. Using these results, the numerical code PLATONggnn has been also constructed, which calculates the reversed process cross section $d\sigma(gg \rightarrow \tilde{\chi}_i^0 \tilde{\chi}_j^0)/d\hat{t}$ for any (\hat{s}, \hat{t}) -values and any MSSM model with real soft breaking parameters [18].

We then compute the LHC cross sections for $PP \rightarrow \tilde{\chi}_i^0 \tilde{\chi}_j^0 + \dots$, by convoluting the gg and $q\bar{q}$ subprocess cross sections, with the corresponding quark and gluon distribution functions in the initial protons P . We then discuss the contributions of both subprocess to several observables (invariant mass, transverse momentum and angular distributions) and we give illustrations for an extensive set of benchmark models in MSSM. As we will see below, depending on the choice of MSSM parameters and the kinematical regions looked at, the one loop $gg \rightarrow \tilde{\chi}_i^0 \tilde{\chi}_j^0$ subprocess may occasionally give comparable or even larger effects, than the tree level $q\bar{q} \rightarrow \tilde{\chi}_i^0 \tilde{\chi}_j^0$ one.

These results imply an interesting complementarity between the future LHC measurements, the related $\gamma\gamma \rightarrow \tilde{\chi}_i^0 \tilde{\chi}_j^0$ measurements at a future Linear Collider and the Dark Matter searches in cosmic experiments.

The contents of the paper is the following. Sect.2 is devoted to the process $q\bar{q} \rightarrow \tilde{\chi}_i^0 \tilde{\chi}_j^0$. The general properties of the helicity amplitudes are studied in the subsection 2.1, where the seven basic independent amplitudes are identified. The tree-level helicity amplitudes and cross sections are subsequently presented in Section 2.2 and Appendix A.1; while the electroweak and SUSY QCD corrections to the helicity amplitudes, at leading and subleading logarithmic accuracy, are given in Section 2.3 and Appendix A.2. In Sect.3, the one loop process $gg \rightarrow \tilde{\chi}_i^0 \tilde{\chi}_j^0$ is presented. Applications to neutralino pair production at LHC using the parton formalism are given in Sect.4, where the numerical results are also discussed. The concluding remarks are given in Sect.5, while the parton model kinematics is detailed in Appendix B.

2 The subprocess $q\bar{q} \rightarrow \tilde{\chi}_i^0 \tilde{\chi}_j^0$

2.1 Generalities about Helicity amplitudes for $q\bar{q} \rightarrow \tilde{\chi}_i^0 \tilde{\chi}_j^0$

For an incoming $q\bar{q}$ -pair, and an outgoing pair of neutralinos, the process is written as

$$q(q_1, \lambda_1) \bar{q}(q_2, \lambda_2) \rightarrow \tilde{\chi}_i^0(p_i, \tau_i) \tilde{\chi}_j^0(p_j, \tau_j) \quad , \quad (1)$$

where (q_1, q_2, p_i, p_j) and $(\lambda_1, \lambda_2, \tau_i, \tau_j)$ are the momenta and helicities of the incoming and outgoing particles. The usual Mandelstam variables for the subprocess are defined as

$$\hat{s} = (q_1 + q_2)^2 = (p_i + p_j)^2 \quad , \quad \hat{t} = (q_1 - p_i)^2 = (q_2 - p_j)^2 \quad , \quad \hat{u} = (q_1 - p_j)^2 = (q_2 - p_i)^2. \quad (2)$$

Since the top quark structure function is vanishing in the proton and the other quarks are not too heavy, the incoming q and \bar{q} in (1) are taken as massless as far as the kinematics

²The possible values of the helicities $\lambda_1, \lambda_2, \tau_i, \tau_j$ are, as usually, taken as $\pm 1/2$.

is concerned, but we keep the potentially large (particularly for the third family) Yukawa contributions to the couplings. Finally (m_i, m_j) denote the $(\tilde{\chi}_i^0, \tilde{\chi}_j^0)$ masses, respectively.

The helicity amplitude for process (1) is denoted as

$$F_{\lambda_1\lambda_2;\tau_i\tau_j}^{ij}(\theta^*) \quad , \quad (3)$$

where θ^* is scattering angle in the c.m. of the subprocess. In these amplitudes, \bar{q} and $\tilde{\chi}_j^0$ are treated as particles No2 in the JW conventions [19]. To consistently take into account the Majorana nature of the neutralinos, we always describe the No1 neutralino $\tilde{\chi}_i^0$ through a positive energy Dirac wave function, while the No2 JW particle $\tilde{\chi}_j^0$ is described through a negative energy one³. Fermi statistics for the final neutralinos then implies⁴

$$F_{\lambda_1\lambda_2;\tau_i\tau_j}^{ij}(\theta^*) = (-1)^{\lambda_1-\lambda_2} F_{\lambda_1\lambda_2;\tau_j\tau_i}^{ji}(\pi - \theta^*) \quad , \quad (4)$$

while CP-invariance, valid for real soft breaking and μ parameters, gives

$$F_{\lambda_1\lambda_2;\tau_i\tau_j}^{ij}(\theta^*) = \eta_i\eta_j F_{-\lambda_2,-\lambda_1;-\tau_j,-\tau_i}^{ji}(\theta^*) \quad , \quad (5)$$

where $\eta_i = \pm 1$ is the CP-eigenvalue of the $\tilde{\chi}_i^0$ -neutralino [21].

On the basis of (4, 5) all $q\bar{q}$ -amplitudes may be expressed in terms of seven basic ones, selected as

$$\begin{aligned} & F_{-++-}^{ij}(\theta^*) \quad , \quad F_{+--+}^{ij}(\theta^*) \quad , \quad F_{-+++}^{ij}(\theta^*) \quad , \quad F_{+---}^{ij}(\theta^*) \quad , \\ & F_{++++}^{ij}(\theta^*) \quad , \quad F_{+--+}^{ij}(\theta^*) \quad , \quad F_{+---}^{ij}(\theta^*) \quad . \end{aligned} \quad (6)$$

The other amplitudes are determined from these through

$$\begin{aligned} F_{-++-}^{ij}(\theta^*) &= -F_{-+++}^{ji}(\pi - \theta^*) \quad , \\ F_{+--+}^{ij}(\theta^*) &= -F_{+---}^{ji}(\pi - \theta^*) \quad , \\ F_{-++-}^{ij}(\theta^*) &= F_{-+++}^{ji}(\theta^*)\eta_i\eta_j \quad , \\ F_{+---}^{ij}(\theta^*) &= F_{+---}^{ji}(\theta^*)\eta_i\eta_j \quad , \\ F_{+--+}^{ij}(\theta^*) &= F_{+--+}^{ji}(\pi - \theta^*) \quad , \\ F_{-+++}^{ij}(\theta^*) &= F_{+---}^{ji}(\theta^*)\eta_i\eta_j \quad , \\ F_{-+++}^{ij}(\theta^*) &= F_{+---}^{ji}(\theta^*)\eta_i\eta_j \quad , \\ F_{+---}^{ij}(\theta^*) &= F_{+---}^{ji}(\theta^*)\eta_i\eta_j \quad , \\ F_{+---}^{ij}(\theta^*) &= F_{+---}^{ji}(\pi - \theta^*)\eta_i\eta_j \quad . \end{aligned} \quad (7)$$

We also note that (4, 5) imply the relations

$$F_{++++}^{ij}(\theta^*) = F_{++++}^{ji}(\pi - \theta^*) \quad ,$$

³The same convention is also followed for the $gg \rightarrow \tilde{\chi}_i^0\tilde{\chi}_j^0$ treated below.

⁴We note that (4), which is induced by the anticommuting nature of the Fermionic fields, does not generally agree with the neutralino (anti)symmetry property assumed in [20].

$$\begin{aligned}
F_{++--}^{ij}(\theta^*) &= F_{++--}^{ji}(\pi - \theta^*) , \\
F_{--++}^{ij}(\theta^*) &= F_{--++}^{ji}(\pi - \theta^*) , \\
F_{----}^{ij}(\theta^*) &= F_{----}^{ji}(\pi - \theta^*) , \\
F_{+---}^{ij}(\theta^*) &= -F_{+---}^{ji}(\pi - \theta^*) , \\
F_{-+++}^{ij}(\theta^*) &= -F_{-+++}^{ji}(\pi - \theta^*) , \\
F_{+----}^{ij}(\theta^*) &= -F_{+----}^{ji}(\pi - \theta^*) , \\
F_{-+---}^{ij}(\theta^*) &= -F_{-+---}^{ji}(\pi - \theta^*) .
\end{aligned} \tag{8}$$

In terms of these helicity amplitudes, the unpolarized differential subprocess cross section may expressed as

$$\frac{d\hat{\sigma}(q\bar{q} \rightarrow \tilde{\chi}_i^0 \tilde{\chi}_j^0)}{d\hat{t}} = \frac{1}{192\pi\hat{s}^2} \left(\frac{1}{2}\right)^{\delta_{ij}} \left[\sum_{\lambda_1, \lambda_2; \tau_i, \tau_j} |F_{\lambda_1, \lambda_2; \tau_i, \tau_j}|^2 \right] , \tag{9}$$

where the kinematics are defined in (2) and (B.11-B.16).

2.2 Born amplitudes and cross sections.

The Born amplitude for the process in (1) contains three diagrams (see Fig.1abc) involving s , t and u channel exchanges and written as [13]

$$\begin{aligned}
F_{\lambda_1 \lambda_2 \tau_i \tau_j}^{ijB} &= F_{\lambda_1 \lambda_2 \tau_i \tau_j}^{ijBs} + F_{\lambda_1 \lambda_2 \tau_i \tau_j}^{ijBt} + F_{\lambda_1 \lambda_2 \tau_i \tau_j}^{ijBu} , \tag{10} \\
F_{\lambda_1 \lambda_2 \tau_i \tau_j}^{ijBs} &= -\frac{e^2}{4s_W^2 c_W^2 (\hat{s} - m_Z^2)} \bar{v}(\bar{q}) \gamma^\mu [g_{qL} P_L + g_{qR} P_R] u(q) \cdot \bar{u}_i \gamma_\mu [N^{ij} P_L - N^{ij*} P_R] v_j , \\
F_{\lambda_1 \lambda_2 \tau_i \tau_j}^{ijBt} &= \sum_n \frac{1}{\hat{t} - \tilde{m}_n^2} \bar{v}(\bar{q}) [A_j^{L*}(\tilde{q}_n) P_R + A_j^{R*}(\tilde{q}_n) P_L] v_j \cdot \bar{u}_i [A_i^L(\tilde{q}_n) P_L + A_i^R(\tilde{q}_n) P_R] u(q) , \\
F_{\lambda_1 \lambda_2 \tau_i \tau_j}^{ijBu} &= -\sum_n \frac{1}{\hat{u} - \tilde{m}_n^2} \bar{v}(\bar{q}) [A_i^{L*}(\tilde{q}_n) P_R + A_i^{R*}(\tilde{q}_n) P_L] u_i \cdot \bar{v}_j^c [A_j^L(\tilde{q}_n) P_L + A_j^R(\tilde{q}_n) P_R] u(q) , \tag{11}
\end{aligned}$$

where the index n refers to the summation over the exchanged L- and R- squarks of the same flavor in the t- and u-channel, $P_{L/R} = (1 \mp \gamma_5)/2$, and (i, j) describe the final neutralinos.

Explicit expressions for the seven basic helicity amplitudes listed in (6), are given in (A.1, A.2, A.3, A.4) in Appendix A.1.

- They involve the L and R Zqq -couplings defined as

$$Zqq \Rightarrow -\frac{e}{2s_W c_W} \gamma^\mu [g_{qL} P_L + g_{qR} P_R] , \tag{12}$$

where

$$g_{qL} = 2I_q^3(1 - 2s_W^2|Q_q|) \quad , \quad g_{qR} = -2s_W^2 Q_q \quad , \tag{13}$$

with I_q^3, Q_q being the isospin and charge of the various q_L -quarks.

- The Z-neutralino couplings satisfying

$$Z\tilde{\chi}_i^0\tilde{\chi}_j^0 \Rightarrow \frac{e}{2s_Wc_W}\gamma^\mu[g_{ijL}P_L + g_{ijR}P_R] \quad (14)$$

with

$$g_{ijL} = N^{ij} \equiv Z_{4i}^{N*}Z_{4j}^N - Z_{3i}^{N*}Z_{3j}^N, \quad g_{ijR} = -N^{ij*}, \quad (15)$$

where Z^N denotes the neutralino mixing matrix in the notation of [22]).

- And the neutralino-quark-squark couplings

$$q\tilde{q}_n\tilde{\chi}_i^0 \Rightarrow A_i^L(\tilde{q}_n)P_L + A_i^R(\tilde{q}_n)P_R, \quad (16)$$

where

$$\begin{aligned} A_i^L(\tilde{u}_L) &= -\frac{e}{3\sqrt{2}s_Wc_W}(Z_{1i}^Ns_W + 3Z_{2i}^Nc_W), & A_i^L(\tilde{u}_R) &= -\frac{em_u}{\sqrt{2}M_Ws_W\sin\beta}Z_{4i}^N \\ A_i^R(\tilde{u}_R) &= \frac{2e\sqrt{2}}{3c_W}Z_{1i}^{N*}, & A_i^R(\tilde{u}_L) &= -\frac{em_u}{\sqrt{2}M_Ws_W\sin\beta}Z_{4i}^{N*} \\ A_i^L(\tilde{d}_L) &= -\frac{e}{3\sqrt{2}s_Wc_W}(Z_{1i}^Ns_W - 3Z_{2i}^Nc_W), & A_i^L(\tilde{d}_R) &= -\frac{em_d}{\sqrt{2}M_Ws_W\cos\beta}Z_{3i}^N \\ A_i^R(\tilde{d}_R) &= -\frac{e\sqrt{2}}{3c_W}Z_{1i}^{N*}, & A_i^R(\tilde{d}_L) &= -\frac{em_d}{\sqrt{2}M_Ws_W\cos\beta}Z_{3i}^{N*} \end{aligned} \quad (17)$$

In (17), ($q = u, d$) refer to the incoming up and down quark (antiquark) of any family⁵, while ($\tilde{q}_n = \tilde{q}_L, \tilde{q}_R$) denote the corresponding squarks. We also note that the mixing matrices Z^N in (15, 17), control the Bino, Wino, Higgsino components of the neutralino in the $Z\tilde{\chi}_i^0\tilde{\chi}_j^0$ and $q\tilde{q}\tilde{\chi}^0$ coupling [22, 21]. Finally, we remark that s -channel Born part $F_{\lambda_1\lambda_2\tau_i\tau_j}^{ijBs}$ gives non-vanishing contributions only for purely higgsino production, whereas the t, u -channel Born parts for purely gaugino.

One can then compute the differential cross section either through (9) and the helicity amplitudes in (A.1, A.2, A.3, A.4), or directly by the trace procedure giving

$$\frac{d\hat{\sigma}(q\bar{q} \rightarrow \tilde{\chi}_i^0\tilde{\chi}_j^0)}{d\hat{t}} = \frac{1}{192\pi\hat{s}^2}\left(\frac{1}{2}\right)^{\delta_{ij}} [I_{ss} + I_{tt} + I_{uu} - 2I_{st} + 2I_{su} - 2I_{tu}] \quad (18)$$

where⁶

$$\begin{aligned} I_{ss} &= \frac{e^4(g_{qL}^2 + g_{qR}^2)}{4s_W^4c_W^4(\hat{s} - m_Z^2)^2} \left\{ N^{ij}N^{ij*}[(m_i^2 - \hat{t})(m_j^2 - \hat{t}) + (m_i^2 - \hat{u})(m_j^2 - \hat{u})] \right. \\ &\quad \left. - [(N^{ij})^2 + (N^{ij*})^2]m_im_j\hat{s} \right\}, \\ I_{tt} &= \sum_{k,l} \frac{(m_i^2 - \hat{t})(m_j^2 - \hat{t})}{(\hat{t} - \tilde{m}_k^2)(\hat{t} - \tilde{m}_l^2)} [A_i^L(\tilde{q}_k)A_i^{L*}(\tilde{q}_l) + A_i^R(\tilde{q}_k)A_i^{R*}(\tilde{q}_l)] [A_j^L(\tilde{q}_k)A_j^{L*}(\tilde{q}_l)] \end{aligned}$$

⁵As usual, we will only consider non-vanishing structure functions for incoming u, d, s, c and b quarks.

⁶Analogous expression for gaugino production in e^-e^+ Colliders have appeared in [23].

$$\begin{aligned}
& + A_j^R(\tilde{q}_k) A_j^{R*}(\tilde{q}_l)] , \\
I_{uu} &= \sum_{k,l} \frac{(m_i^2 - \hat{u})(m_j^2 - \hat{u})}{(\hat{u} - \tilde{m}_k^2)(\hat{u} - \tilde{m}_l^2)} [A_i^{L*}(\tilde{q}_k) A_i^L(\tilde{q}_l) + A_i^{R*}(\tilde{q}_k) A_i^R(\tilde{q}_l)] [A_j^{L*}(\tilde{q}_k) A_j^L(\tilde{q}_l) \\
& + A_j^{R*}(\tilde{q}_k) A_j^R(\tilde{q}_l)] , \\
I_{st} &= \sum_k \frac{e^2}{2s_W^2 c_W^2 (\hat{t} - \tilde{m}_k^2)(\hat{s} - m_Z^2)} \text{Re} \left\{ [N^{ij*} g_{qR} A_i^R(\tilde{q}_k) A_j^{R*}(\tilde{q}_k) - N^{ij} g_{qL} A_i^L(\tilde{q}_k) A_j^{L*}(\tilde{q}_k)] \right. \\
& \cdot (m_i^2 - \hat{t})(m_j^2 - \hat{t}) + [N^{ij*} g_{qL} A_i^L(\tilde{q}_k) A_j^{L*}(\tilde{q}_k) - N^{ij} g_{qR} A_i^R(\tilde{q}_k) A_j^{R*}(\tilde{q}_k)] m_i m_j \hat{s} \left. \right\} , \\
I_{su} &= \sum_k \frac{e^2}{2s_W^2 c_W^2 (\hat{u} - \tilde{m}_k^2)(\hat{s} - m_Z^2)} \text{Re} \left\{ [N^{ij*} g_{qL} A_i^{L*}(\tilde{q}_k) A_j^L(\tilde{q}_k) - N^{ij} g_{qR} A_i^{R*}(\tilde{q}_k) A_j^R(\tilde{q}_k)] \right. \\
& \cdot (m_i^2 - \hat{u})(m_j^2 - \hat{u}) + [N^{ij*} g_{qR} A_i^{R*}(\tilde{q}_k) A_j^R(\tilde{q}_k) - N^{ij} g_{qL} A_i^{L*}(\tilde{q}_k) A_j^L(\tilde{q}_k)] m_i m_j \hat{s} \left. \right\} \\
I_{tu} &= \sum_{k,l} \frac{1}{(\hat{u} - \tilde{m}_l^2)(\hat{t} - \tilde{m}_k^2)} \text{Re} \left\{ [A_i^L(\tilde{q}_k) A_i^L(\tilde{q}_l) A_j^{L*}(\tilde{q}_k) A_j^{L*}(\tilde{q}_l) \right. \\
& + A_i^R(\tilde{q}_k) A_i^R(\tilde{q}_l) A_j^{R*}(\tilde{q}_k) A_j^{R*}(\tilde{q}_l)] m_i m_j \hat{s} + \frac{1}{2} [A_i^{L*}(\tilde{q}_k) A_i^{R*}(\tilde{q}_l) A_j^R(\tilde{q}_k) A_j^L(\tilde{q}_l) \\
& + A_i^{R*}(\tilde{q}_k) A_i^{L*}(\tilde{q}_l) A_j^L(\tilde{q}_k) A_j^R(\tilde{q}_l)] [(m_i^2 - \hat{t})(m_j^2 - \hat{t}) + (m_i^2 - \hat{u})(m_j^2 - \hat{u}) \\
& \left. - \hat{s}(\hat{s} - m_i^2 - m_j^2)] \right\} , \tag{19}
\end{aligned}$$

where m_i , m_j are the neutralino masses and N^{ij} are defined in (15).

The results in eq.(18) disagree with those of [20], where symmetry properties of the $\tilde{\chi}_i^0 \tilde{\chi}_j^0$ states which are different from those in (4) have been used.

2.3 One loop electroweak and SUSY QCD corrections to $q\bar{q} \rightarrow \tilde{\chi}_i^0 \tilde{\chi}_j^0$

In principle, one loop EW corrections for $q\bar{q} \rightarrow \tilde{\chi}_i^0 \tilde{\chi}_j^0$ should be taken into account, particularly because the energy reach at LHC is so big, that the large logarithmic contributions to the amplitudes may reach the few tens of percent level [14, 15, 16]. In the models we have considered, this implies a reduction of the cross sections sometimes by almost a factor of two, while preserving their shape. Since the non-logarithmic one-loop contributions seem to lie at the few percent level, which is also the level of the expected experimental accuracy, it may be adequate to ignore these difficult to calculate effects in $(q\bar{q} \rightarrow \tilde{\chi}_i^0 \tilde{\chi}_j^0)$ at LHC energies.

In this section we present therefore, the leading and subleading EW logarithmic contributions to the $q\bar{q} \rightarrow \tilde{\chi}_i^0 \tilde{\chi}_j^0$ helicity amplitudes, following [14, 15, 16], where applications for LC and LHC have been given. They are separated into three types of terms which are:

- Universal electroweak (EW) terms. These are process-independent terms appearing as correction factors to the Born amplitude. They consist of "gauge" and "Yukawa" contributions associated to each external line and determined by its quantum numbers and chirality. Their expressions for a quark or neutralino line are respectively determined as follows:

External quark line of chirality $a = L, R$: Since all quarks are taken as massless as far as the kinematics are concerned⁷, the quark lines correspond to a definite chirality a . The induced correction then is

$$F_a^{ijB} \cdot [c(q)_a] \ , \quad (20)$$

where F_a^{ijB} describes the corresponding Born amplitude from (10) involving an external quark line of chirality a (which at high energies is essentially equivalent to the helicity), while (i, j) -count the mass eigenstates of the neutralinos. The coefficient in (20) is written as

$$c(q)_a = c(q, \text{gauge})_a + c(q, \text{yuk})_a \ , \quad (21)$$

with the gauge contribution being

$$c(q, \text{gauge})_a = \frac{\alpha}{8\pi} \left[\frac{I_q(I_q + 1)}{s_W^2} + \frac{Y_q^2}{4c_W^2} \right] \left(2 \ln \frac{\hat{s}}{m_W^2} - \ln^2 \frac{\hat{s}}{m_W^2} \right) \ , \quad (22)$$

where I_q is the full isospin of the quark q_a with chirality $a = L$ or R , and $Y_q = 2(Q_q - I_q^{(3)})$ defines its hypercharge in terms of the third isospin component $I_q^{(3)}$. Correspondingly, the Yukawa term (for b, t quarks only) is

$$c(q, \text{yuk})_a = -\frac{\alpha}{16\pi s_W^2} \left[\ln \frac{\hat{s}}{m_W^2} \right] \left\{ \left[\frac{m_t^2}{m_W^2 \sin^2 \beta} + \frac{m_b^2}{m_W^2 \cos^2 \beta} \right] \delta_{aL} + 2 \left[\frac{m_b^2}{m_W^2 \cos^2 \beta} \delta_{I_q^{(3)}, -1/2} + \frac{m_t^2}{m_W^2 \sin^2 \beta} \delta_{I_q^{(3)}, 1/2} \right] \delta_{aR} \right\} \ . \quad (23)$$

We note that an external antiquark line should be counted separately giving an additional contribution determined by the same formulae (20-23). Moreover, the same formulae describe also the logarithmic contributions associated with each external squark, anti-squark, lepton or slepton line [14, 15, 16].

For an external neutralino line of chirality b , it is convenient to use a matrix notation

$$\sum_k \left[F_b^{ikB} c(\tilde{\chi}_k^0 \tilde{\chi}_j^0)_b + F_b^{kjB} c^*(\tilde{\chi}_k^0 \tilde{\chi}_i^0)_b \right] \ , \quad (24)$$

and to separate the higgsino from the gaugino components of the matrix elements:

$$c(\tilde{\chi}_l^0 \tilde{\chi}_{l'}^0)_b = c(\tilde{\chi}_l^0 \tilde{\chi}_{l'}^0 \text{ higgsino, gauge})_b + c(\tilde{\chi}_l^0 \tilde{\chi}_{l'}^0 \text{ higgsino, yuk})_b + c(\tilde{\chi}_l^0 \tilde{\chi}_{l'}^0 \text{ gaugino, gauge})_b \ , \quad (25)$$

⁷The large third family Yukawa terms appear only as couplings and do not concern the kinematics.

with

$$\begin{aligned}
c(\tilde{\chi}_l^0 \tilde{\chi}_{l'}^0 \text{ higgsino, gauge})_b &= \frac{\alpha(1 + 2c_W^2)}{32\pi s_W^2 c_W^2} \left(2 \ln \frac{\hat{s}}{m_W^2} - \ln^2 \frac{\hat{s}}{m_W^2} \right) \\
&\cdot \left[(Z_{4l}^{N*} Z_{4l'}^N + Z_{3l}^{N*} Z_{3l'}^N) \delta_{bL} + (Z_{4l}^N Z_{4l'}^{N*} + Z_{3l}^N Z_{3l'}^{N*}) \delta_{bR} \right], \\
c(\tilde{\chi}_l^0 \tilde{\chi}_{l'}^0 \text{ higgsino, yuk})_b &= -\frac{3\alpha}{16\pi s_W^2 m_W^2} \left[\ln \frac{\hat{s}}{m_W^2} \right] \\
&\cdot \left[\frac{m_t^2}{\sin^2 \beta} (Z_{4l}^{N*} Z_{4l'}^N \delta_{bL} + Z_{4l}^N Z_{4l'}^{N*} \delta_{bR}) + \frac{m_b^2}{\cos^2 \beta} (Z_{3l}^{N*} Z_{3l'}^N \delta_{bL} + Z_{3l}^N Z_{3l'}^{N*} \delta_{bR}) \right], \\
c(\tilde{\chi}_l^0 \tilde{\chi}_{l'}^0 \text{ gaugino, gauge})_b &= -\frac{\alpha}{4\pi s_W^2} \left[Z_{2l}^{N*} Z_{2l'}^N P_L + Z_{2l}^N Z_{2l'}^{N*} P_R \right] \left[\ln^2 \frac{\hat{s}}{m_W^2} \right]. \quad (26)
\end{aligned}$$

The logarithmic contributions associated to the purely higgsino s-channel Born amplitude F_b^{ikBs} of⁸ Fig.1a only involve the "higgsino, gauge" and "higgsino, Yukawa" elements, whereas the contributions associated to the purely gaugino t- and u- Born amplitudes $F_b^{ikBt,u}$, only involve the "gaugino, gauge" elements.

- Angular and process dependent terms. They originate from diagrams involving W internal lines supplying soft-infrared $\ln^2 t$ or $\ln^2 u$ terms. Diagrams with internal Z lines are negligible, since their contributions turn out to be orthogonal to the Born terms and cannot interfere with them. The contributing diagrams therefore consist of boxes with an intermediate WW pair in the s-channel, triangles involving a single W connected to a squark exchange in the t or u channels, and boxes involving a single W and a squark in the t or u channels.
- Renormalization Group (RG) terms. They arise from intermediate Z boson Born terms contributing to Higgsino production only and inducing running effects to the corresponding g and g' gauge couplings; see Fig.1a. In terms of the s-channel Born amplitudes of (10), they are written as

$$F^{RG} = -\frac{1}{4\pi^2} \left(g^4 \tilde{\beta}_0 \frac{dF^{ijBs}}{dg^2} + g'^4 \tilde{\beta}'_0 \frac{dF^{ijBs}}{dg'^2} \right) \left[\ln \frac{\hat{s}}{\mu^2} \right], \quad (27)$$

where $g^2 = e^2/s_W^2$, $g'^2 = e^2/c_W^2$,

$$\tilde{\beta}_0 = \frac{3}{4}C_A - \frac{n_g}{2} - \frac{n_h}{8} = -\frac{1}{4}, \quad \tilde{\beta}'_0 = -\frac{5}{6}n_g - \frac{n_h}{8} = -\frac{11}{4} \quad (28)$$

and $C_A = 2$, $n_g = 3$, $n_h = 2$ in MSSM. Applying this procedure to the 7 basic Born helicity amplitudes of Appendix A.1, implies the substitutions

$$\begin{aligned}
\frac{e^2 g_{qL}}{s_W^2 c_W^2} &\rightarrow -\frac{(2I_{qL}^{(3)})}{4\pi^2} \left[\ln \frac{\hat{s}}{\mu^2} \right] \{ \tilde{\beta}_0 g^4 + \tilde{\beta}'_0 g'^4 [1 - 2|Q_q|] \}, \\
\frac{e^2 g_{qR}}{s_W^2 c_W^2} &\rightarrow \frac{(2Q_q)}{4\pi^2} \left[\ln \frac{\hat{s}}{\mu^2} \right] \{ \tilde{\beta}'_0 g'^4 \}, \quad (29)
\end{aligned}$$

⁸See also (10).

The resulting expression for the seven basic helicity amplitudes of (6), are given in Appendix A.2. For what concerns the magnitude of the various corrections, the following general comments can be made. In the LHC domain (say for $\sqrt{\hat{s}} \simeq 1$ TeV) a single $\ln(\hat{s}/m_W^2)$ and a squared $\ln^2(\hat{s}/m_W^2)$ give enhancement factors of about 5 and 25, respectively. So one expects that the corrections are of the order of -5% for the quark or higgsino-gauge terms, -25% for the gaugino gauge ones, and -10% for the higgsino-Yukawa terms (depending on $\tan\beta$ value). The angular dependent terms have a more complicated structure; their sign is not fixed, while their magnitude can reach the 10% level. The addition of these various electroweak terms is strongly model dependent, especially due to the Z_{ij}^N matrix elements controlling the amount of the higgsino and gaugino components of the neutralinos. The net EW effect on the amplitude though, is essentially always negative and can easily reach the several tens of percent level.

The logarithmic SUSY QCD corrections for quark-antiquark processes at order α_s are given by [17, 16],

$$F_{\lambda_q, \lambda_{\bar{q}}; \tau_i, \tau_j}^{SUSY QCD} = F_{\lambda_q, \lambda_{\bar{q}}; \tau_i, \tau_j}^{Born} \left[-\frac{\alpha_s}{3\pi} \ln \frac{\hat{s}}{M^2} \right]. \quad (30)$$

This simple logarithmic terms arise from diagrams containing virtual squarks and gluinos interacting via SUSY QCD couplings; such diagrams produce no $\ln^2 s$ -terms. By itself this single log term is of course negative, and it would remain around -5% in the observable LHC domain. In addition to these though, we should always also consider the pure QCD leading and next-to-leading mass dependent corrections which, as shown in ref.[17], result into a K factor that turns out to be positive and of the order of 30%. These later corrections are not discussed in the present paper.

3 The one loop process $gg \rightarrow \tilde{\chi}_i^0 \tilde{\chi}_j^0$

This process first appears at the one loop level through the triangle and box diagrams fully listed in [6]. These diagrams basically involve gluon-quark-squark and neutralino-chargino-squark couplings; no gluino can appear at this order. Accidental degeneracies between the neutralino masses and squark masses can give some enhancement effects. In addition, single Z , h^0 , H^0 or A^0 exchanges in the s-channel, can also give enhancements and resonance effects at the corresponding c.m. energies. These situations are rather similar to those already mentioned for the $\gamma\gamma \rightarrow \tilde{\chi}_i^0 \tilde{\chi}_j^0$ process in [7].

The helicity amplitudes for the process

$$g(q_1, \mu_1)g(q_2, \mu_2) \rightarrow \tilde{\chi}_i^0(p_i, \tau_i)\tilde{\chi}_j^0(p_j, \tau_j), \quad (31)$$

are denoted as

$$F_{\mu_1 \mu_2; \tau_i \tau_j}^{ij}(\theta^*), \quad (32)$$

where the momenta and helicities of the incoming gluons and outgoing neutralinos are defined, and θ^* again denotes the c.m. scattering angle. We use the same $(\tilde{\chi}_i^0, \tilde{\chi}_j^0)$

conventions as in the $q\bar{q}$ case and in [7], implying

$$F_{\mu_1, \mu_2; \tau_i, \tau_j}^{ij}(\theta^*) = (-1)^{\mu_1 - \mu_2} F_{\mu_1, \mu_2; \tau_j, \tau_i}^{ji}(\pi - \theta^*) \quad (33)$$

from $\tilde{\chi}_i^0 \tilde{\chi}_j^0$ fermion-antisymmetry, and

$$F_{\mu_1, \mu_2; \tau_i, \tau_j}^{ij}(\theta^*) = (-1)^{\tau_i - \tau_j} F_{\mu_2, \mu_1; \tau_i, \tau_j}^{ji}(\pi - \theta^*) \quad (34)$$

from gg -boson symmetry.

If the MSSM breaking parameters and the Higgs parameter μ are real, then CP invariance holds, implying

$$F_{-\mu_1, -\mu_2; -\tau_i, -\tau_j}^{ij}(\theta^*) = (-1)^{\tau_i - \tau_j - (\mu_1 - \mu_2)} \eta_i \eta_j F_{\mu_1, \mu_2; \tau_i, \tau_j}^{ij}(\theta^*) \quad , \quad (35)$$

where $\eta_i, \eta_j = \pm 1$ are the CP-eigenvalues of the two produced neutralinos⁹. In such a case, time inversion invariance implies the same helicity amplitudes for the process (31) and its inverse. Combining (33, 34, 35), we get

$$F_{\mu_1 \mu_2; \tau_i \tau_j}^{ij}(\theta^*) = (-1)^{\mu_1 - \mu_2 + \tau_j - \tau_i} F_{\mu_2 \mu_1; \tau_j \tau_i}^{ji}(\theta^*) = \eta_i \eta_j \tilde{F}_{-\mu_2, -\mu_1; -\tau_j, -\tau_i}^{ji}(\theta^*) \quad , \quad (36)$$

where the first part comes from (33, 34) alone, while for the last part the CP-invariance relation (35) is also used.

In terms of these helicity amplitudes, the unpolarized differential subprocess cross section is

$$\frac{d\hat{\sigma}(gg \rightarrow \tilde{\chi}_i \tilde{\chi}_j)}{d\hat{t}} = \frac{1}{4096\pi \hat{s}^2} \left(\frac{1}{2}\right)^{\delta_{ij}} \sum_{\mu_1 \mu_2 \tau_i \tau_j} |F_{\mu_1 \mu_2 \tau_i \tau_j}|^2. \quad (37)$$

Together with the present paper, we release in [18] the numerical code PLATONggm, which calculates the differential cross section (37) as a functions of θ^* and \hat{s} , for any set of real SUSY parameters at the electroweak scale.

The above amplitudes are basically of order α_s/π weaker than the tree level $q\bar{q}$ amplitudes of the preceding Section. In certain SUSY models though, this reduction can be partially compensated by the aforementioned enhancement factors. But in practice, the most important feature at LHC is the relative size of gg and $q\bar{q}$ distribution functions inside the proton; *i.e.* the fact that at "low" subenergies the gg fluxes are much larger than $q\bar{q}$ ones. Because of this, and as we see in Section 4, there are benchmark models where the gg contribution to neutralino-neutralino production at LHC, is larger than the $q\bar{q}$ one.

4 $\tilde{\chi}_i^0 \tilde{\chi}_j^0$ distributions in Proton-Proton collisions

In this section we discuss numerical results for the process $PP \rightarrow \tilde{\chi}_i^0 \tilde{\chi}_j^0 + \dots$ at LHC (c.m. energy $\sqrt{s} = 14$ TeV) generated by the subprocesses $gg, q\bar{q} \rightarrow \tilde{\chi}_i^0 \tilde{\chi}_j^0$; ($\tilde{\chi}_i^0$ is always taken

⁹We follow the same notation as in *e.g.* [21].

heavier than $\tilde{\chi}_j^0$). All necessary formulae describing the kinematics for two massive final particles are presented in Appendix B. These allow the computation of the neutralino-pair invariant mass distributions $d\sigma/d\hat{s}$, the transverse energy distribution of the heavier neutralino $d\sigma/dx_{T_i}$, and the angular distribution in the neutralino-neutralino center of mass $d\sigma/d\chi_i$ described through χ_i defined in (B.19); compare the formalisms in Sections B.2.3, B.2.1 and B.2.4 respectively.

The present formalism allows of course to compute any $\tilde{\chi}_i^0\tilde{\chi}_j^0$ channel for any MSSM model with real soft breaking and μ parameters, using code PLATONggnn released in [18]. In this paper we also assumed that the $\tilde{\chi}_1^0$ escapes the detector without being observed¹⁰, so that the identification of *e.g.* the $\tilde{\chi}_2^0\tilde{\chi}_1^0$ -production is only done through the detection of $\tilde{\chi}_2^0$. Our illustrations are restricted to the $\tilde{\chi}_2^0\tilde{\chi}_1^0$ and $\tilde{\chi}_2^0\tilde{\chi}_2^0$ channels.

As an example, for the quark and gluon distribution functions inside the proton we use the MRST2003c package [11] at the scale (B.30). Using this and the 31 benchmark models [8, 9, 10] already considered in the previous papers¹¹ [6, 7], we have made numerical computations of the above three single variable distributions. Two main features come out from this study.

At high invariant subprocess energies (close to 1 TeV), the gg contribution becomes negligible compared to the $q\bar{q}$ -ones. This is due to two effects; the gg subprocess cross section is reduced by the one loop factor α_s/π compared to the tree level $q\bar{q}$ -subprocess, while the gg luminosity is comparable to (or even weaker than) the $q\bar{q}$ one.

On the opposite energy site, within a few hundreds of GeV above threshold, the gg flux may be so large, that the gg contribution may compete or even overpass the $q\bar{q}$ -contribution by a factor of 10 or more in some of the benchmark models. This is further enhanced in cases where the A^0 or H^0 Higgs boson can couple to $\tilde{\chi}_2^0\tilde{\chi}_1^0$ or $\tilde{\chi}_2^0\tilde{\chi}_2^0$ channels.

For the illustrations presented here, we have mainly selected those of the benchmark models mentioned above where the competition between the gg and $q\bar{q}$ contributions is most spectacular. Thus, in Figs.2-5 we show the invariant mass distribution $d\sigma/d\hat{s}$ in the cases where there is a resonant enhancement in the gg contribution (models SPS1a1, SPS5, SPS6, SPS8, [8]), while in Figs.6, 7 the gg contribution is smooth but important at low subenergies (models SPS7, CDG24, [8, 10]), and it is further reduced in¹² SPS4 (Fig.8).

In all cases, one sees that the gg contribution to $d\sigma/d\hat{s}$ has a larger slope than the $q\bar{q}$ contribution; the effect being mainly due to the behavior of the gluon distribution functions. The precise magnitude of the gg contribution is however strongly model dependent and arises as the result of many features of the SUSY spectrum involved in the one loop diagrams contributing to $gg \rightarrow \tilde{\chi}_i^0\tilde{\chi}_j^0$ [6].

As already discussed at the end of Sect.2.3, the one loop logarithmic electroweak corrections to $q\bar{q} \rightarrow \tilde{\chi}_i^0\tilde{\chi}_j^0$ tend to reduce the size of the $q\bar{q}$ tree level cross sections; see also [14, 15, 16]. They are strongly model dependent (due to the neutralino mixing matrix

¹⁰This would be the case if $\tilde{\chi}_1^0$ is the stable LSP.

¹¹The high scale values of the defining parameters of these models are listed in Tables 1,2,3 of [6].

¹²The gg contribution may become even smaller in some of the other benchmark models mentioned above.

and $\tan\beta$), and can reach several tens percent for the amplitudes. For certain models, the addition of the various terms can lead to a reduction of the size of the $q\bar{q}$ cross sections by almost a factor two, but they do not strongly modify their shapes. This reduction will of course be somewhat reduced by the enhancements induced by the pure QCD effects [17], but it is nevertheless sufficient to increase the relative importance of the gg contribution.

The features observed in the $d\sigma/d\hat{s}$ distributions of Figs.2-8, can also be seen in the transverse energy distributions $d\sigma/dx_{T_i}$. In order to not multiply the number of figures, we only give illustrations of this fact for two typical models, SPS1a in Fig.9 (where there is a resonance), and SPS7 in Fig.10 (where there is no resonance).

Finally we have examined the distribution $d\sigma/d\chi_i$, which is essentially controlled by the neutralino-neutralino center of mass angular distribution; *i.e.* the $\cos\theta^*$ dependence discussed in Appendix B2.4 and (B.19). Such χ_i distributions can also be used as a complementary test of the dynamics responsible for neutralino-neutralino production. Typical illustrations for models SPS1a and SPS7 appear in Fig.11 and Fig.12 respectively. Concerning them we should remark, that the EW correction to the $q\bar{q}$ subprocess are reliable mainly in large χ_i region, where the gg subprocess may also be important, especially if there is an A^0 or H^0 resonance effect. This appears as a threshold effect corresponding to the value of χ_i above which the mass of the resonance lies within the allowed integration domain for (B.43). On the contrary, the large correction in the small χ_i range of Figs.11,12 should not be taken too seriously, since it is caused from a region where $|t|$ is small and the leading-log predictions not valid.

5 Final discussion

In this paper we have considered the neutralino pair production processes in proton-proton collisions at LHC. In the description we have taken into account the subprocess $q\bar{q} \rightarrow \tilde{\chi}_i^0 \tilde{\chi}_j^0$ calculated at the Born level as a first option, and as a second option we have included also leading and subleading logarithmic corrections. The genuine one loop $gg \rightarrow \tilde{\chi}_i^0 \tilde{\chi}_j^0$ subprocess, is fully taken into account. The description applies to any MSSM model with real soft breaking and μ parameters. Analytic expressions for the helicity amplitudes have been explicitly written for $q\bar{q}$ -subprocess, while a numerical code PLATONggnn is released allowing the computation of the rather involved $d\hat{\sigma}(gg \rightarrow \tilde{\chi}_i^0 \tilde{\chi}_j^0)/d\hat{t}$, for any neutralino pair [18].

After convoluting the subprocess cross sections with parton distribution functions, several observable distributions in $PP \rightarrow \tilde{\chi}_i^0 \tilde{\chi}_j^0 + \dots$ at LHC, have been studied. For the applications, we have restricted to $\tilde{\chi}_2^0 \tilde{\chi}_1^0$ and $\tilde{\chi}_2^0 \tilde{\chi}_2^0$ production in the context of 31 benchmarks MSSM models also considered in [6, 7]. A strong model dependence is observed, to which almost all aspects of the MSSM spectrum contribute through masses and mixing matrix elements.

One of the most striking feature we have found is the important role of the gg subprocesses, which, although basically suppressed by the one loop α_s/π factor, it may occasionally supply a larger contribution than the $q\bar{q}$ subprocess. This may occur close

to and slightly above threshold, where the gg luminosity could be sufficiently large to compensate for the α_s/π factor. In some models, the one loop gg amplitudes may be further enhanced by the presence of A^0 or H^0 Higgs boson resonances, and possibly also by accidental degeneracies between the neutralino and squark masses.

We have also given detail illustrations for the invariant mass, transverse energy and angular distributions, for the case of seven benchmark models where the gg contribution is generally spectacular [8, 9, 10]; *i.e.* appearance of peaks, threshold effects etc. In the few hundred GeV subenergy domain, such structures of the $d\sigma/d\hat{s}$ distributions, appear in the range of 1 to 100 fb/TeV⁻² and should be observable at LHC. This may also be true for the $d\sigma/dx_{Ti}$ and $d\sigma/d\chi_i$ distributions; compare Figs.9-11. We should remember though, that there exist benchmark models also, where the gg contribution is rather marginal, as *e.g.* in model SPS4 [8] and others [9, 10].

In all cases, the effect of the one loop logarithmic corrections to the $q\bar{q}$ cross sections appear to be at the few tens of percent level or more, compared to the tree contribution, and should be taken into account in LHC computations.

These features make the neutralino pair production processes rather interesting for testing the SUSY dynamics at LHC. The reason is that they provide tests which will be complementary to those addressing the cascade decays of initially produced colored SUSY particles to eventually $\tilde{\chi}_1^0$, which is here assumed to be the LSP; *e.g.* studies of mass spectra and decay branching ratios [2]. In particular, consistency checks should thus become available, allowing the strengthening of possible constraints on the validity of specific models.

Moreover, in such neutralino pair production, the role of the Majorana nature of the final state particles is more prominent than in decays involving just one neutralino at a time. Since no such states (except possible the neutrinos) have been observed in the past, it would be interesting to have eventually some experimental support of our understanding of the Majorana nature.

If $\tilde{\chi}_1^0$ turns out to be an important or dominant component Dark Matter, the present calculations¹³, should also help in providing LHC constraints on the direct or indirect observations of the Dark Matter properties, whenever they will become available.

¹³For the same reason, Linear Collider studies should also be helpful [7].

Appendix A

A.1 Tree level helicity amplitudes for $q\bar{q} \rightarrow \tilde{\chi}_i^0 \tilde{\chi}_j^0$

Using the notation of (10), the Born contributions arising from the s-channel diagram in Fig.1a, to the seven basic helicity amplitudes listed in (6) consist of

$$\begin{aligned}
F_{-++-}^{ijBs} &= \frac{e^2 g_{qL} \sqrt{\hat{s}}}{8s_W^2 c_W^2 (\hat{s} - m_Z^2)} (1 + \cos \theta^*) \left[\sqrt{\hat{s} - (m_i - m_j)^2} (N^{ij} - N^{ij*}) \right. \\
&\quad \left. + \sqrt{\hat{s} - (m_i + m_j)^2} (N^{ij} + N^{ij*}) \right] , \\
F_{+-+-}^{ijBs} &= \frac{e^2 g_{qR} \sqrt{\hat{s}}}{8s_W^2 c_W^2 (\hat{s} - m_Z^2)} (1 + \cos \theta^*) \left[\sqrt{\hat{s} - (m_i - m_j)^2} (N^{ij} - N^{ij*}) \right. \\
&\quad \left. - \sqrt{\hat{s} - (m_i + m_j)^2} (N^{ij} + N^{ij*}) \right] , \\
F_{-+++}^{ijBs} &= \frac{e^2 g_{qL}}{8s_W^2 c_W^2 (\hat{s} - m_Z^2)} \sin \theta^* \left[\sqrt{\hat{s} - (m_i - m_j)^2} (m_i + m_j) (N^{ij} - N^{ij*}) \right. \\
&\quad \left. + \sqrt{\hat{s} - (m_i + m_j)^2} (m_i - m_j) (N^{ij} + N^{ij*}) \right] , \\
F_{++++}^{ijBs} &= -\frac{e^2 g_{qR}}{8s_W^2 c_W^2 (\hat{s} - m_Z^2)} \sin \theta^* \left[\sqrt{\hat{s} - (m_i - m_j)^2} (m_i + m_j) (N^{ij} - N^{ij*}) \right. \\
&\quad \left. + \sqrt{\hat{s} - (m_i + m_j)^2} (m_i - m_j) (N^{ij} + N^{ij*}) \right] , \tag{A.1}
\end{aligned}$$

while

$$F_{++\tau_i\tau_j}^{ijBs} = F_{--\tau_i\tau_j}^{ijBs} = 0 , \tag{A.2}$$

for all (τ_i, τ_j) -values¹⁴. Here θ^* is the scattering angle in the c.m. of the subprocess, and Z^N denotes the neutralino mixing matrix in the notation of [22].

The Born contributions to the seven basic helicity amplitudes of (6), arising from the t-channel diagram in Fig.1b, are

$$\begin{aligned}
F_{-++-}^{ijBt} &= -\frac{\sqrt{\hat{s}}}{4} \left[\sqrt{\hat{s} - (m_i - m_j)^2} - \sqrt{\hat{s} - (m_i + m_j)^2} \right] \\
&\quad \cdot \sum_n \left(\frac{1}{\hat{t} - \tilde{m}_n^2} A_i^L(\tilde{q}_n) A_j^{L*}(\tilde{q}_n) \right) (1 + \cos \theta^*) , \\
F_{+-+-}^{ijBt} &= -\frac{\sqrt{\hat{s}}}{4} \left[\sqrt{\hat{s} - (m_i - m_j)^2} - \sqrt{\hat{s} - (m_i + m_j)^2} \right] \\
&\quad \cdot \sum_n \left(\frac{1}{\hat{t} - \tilde{m}_n^2} A_i^R(\tilde{q}_n) A_j^{R*}(\tilde{q}_n) \right) (1 + \cos \theta^*) ,
\end{aligned}$$

¹⁴In fact, the s-channel Born contributions vanish for all amplitudes with equal incoming helicities.

$$\begin{aligned}
F_{-++++}^{ijBt} &= -\frac{1}{4} \left[(m_i + m_j) \sqrt{\hat{s} - (m_i - m_j)^2} - (m_i - m_j) \sqrt{\hat{s} - (m_i + m_j)^2} \right] \\
&\quad \cdot \sum_n \left(\frac{1}{\hat{t} - \tilde{m}_n^2} A_i^L(\tilde{q}_n) A_j^{L*}(\tilde{q}_n) \right) \sin \theta^* , \\
F_{+----}^{ijBt} &= \frac{1}{4} \left[(m_i + m_j) \sqrt{\hat{s} - (m_i - m_j)^2} + (m_i - m_j) \sqrt{\hat{s} - (m_i + m_j)^2} \right] \\
&\quad \cdot \sum_n \left(\frac{1}{\hat{t} - \tilde{m}_n^2} A_i^R(\tilde{q}_n) A_j^{R*}(\tilde{q}_n) \right) \sin \theta^* , \\
F_{++++}^{ijBt} &= -\frac{\sqrt{\hat{s}}}{4} \left[\sqrt{\hat{s} - (m_i - m_j)^2} - \sqrt{\hat{s} - (m_i + m_j)^2} \right] \\
&\quad \cdot \sum_n \left(\frac{1}{\hat{t} - \tilde{m}_n^2} A_i^R(\tilde{q}_n) A_j^{L*}(\tilde{q}_n) \right) (1 + \cos \theta^*) , \\
F_{++--}^{ijBt} &= \frac{\sqrt{\hat{s}}}{4} \left[\sqrt{\hat{s} - (m_i - m_j)^2} + \sqrt{\hat{s} - (m_i + m_j)^2} \right] \\
&\quad \cdot \sum_n \left(\frac{1}{\hat{t} - \tilde{m}_n^2} A_i^R(\tilde{q}_n) A_j^{L*}(\tilde{q}_n) \right) (1 - \cos \theta^*) , \\
F_{++++-}^{ijBt} &= -\frac{1}{4} \left[(m_i + m_j) \sqrt{\hat{s} - (m_i - m_j)^2} + (m_i - m_j) \sqrt{\hat{s} - (m_i + m_j)^2} \right] \\
&\quad \cdot \sum_n \left(\frac{1}{\hat{t} - \tilde{m}_n^2} A_i^R(\tilde{q}_n) A_j^{L*}(\tilde{q}_n) \right) \sin \theta^* , \tag{A.3}
\end{aligned}$$

while the corresponding contributions by the u-channel diagram in Fig.1c, are

$$\begin{aligned}
F_{-++++}^{ijBu} &= \frac{\sqrt{\hat{s}}}{4} \left[\sqrt{\hat{s} - (m_i - m_j)^2} + \sqrt{\hat{s} - (m_i + m_j)^2} \right] \\
&\quad \cdot \sum_n \left(\frac{1}{\hat{u} - \tilde{m}_n^2} A_j^L(\tilde{q}_n) A_i^{L*}(\tilde{q}_n) \right) (1 + \cos \theta^*) , \\
F_{+----}^{ijBu} &= \frac{\sqrt{\hat{s}}}{4} \left[\sqrt{\hat{s} - (m_i - m_j)^2} + \sqrt{\hat{s} - (m_i + m_j)^2} \right] \\
&\quad \cdot \sum_n \left(\frac{1}{\hat{u} - \tilde{m}_n^2} A_j^R(\tilde{q}_n) A_i^{R*}(\tilde{q}_n) \right) (1 + \cos \theta^*) , \\
F_{-++++}^{ijBu} &= \frac{1}{4} \left[(m_i + m_j) \sqrt{\hat{s} - (m_i - m_j)^2} + (m_i - m_j) \sqrt{\hat{s} - (m_i + m_j)^2} \right] \\
&\quad \cdot \sum_n \left(\frac{1}{\hat{u} - \tilde{m}_n^2} A_j^L(\tilde{q}_n) A_i^{L*}(\tilde{q}_n) \right) \sin \theta^* , \\
F_{+----}^{ijBu} &= -\frac{1}{4} \left[(m_i + m_j) \sqrt{\hat{s} - (m_i - m_j)^2} - (m_i - m_j) \sqrt{\hat{s} - (m_i + m_j)^2} \right] \\
&\quad \cdot \sum_n \left(\frac{1}{\hat{u} - \tilde{m}_n^2} A_j^R(\tilde{q}_n) A_i^{R*}(\tilde{q}_n) \right) \sin \theta^* ,
\end{aligned}$$

$$\begin{aligned}
F_{++++}^{ijBu} &= -\frac{\sqrt{\hat{s}}}{4} \left[\sqrt{\hat{s} - (m_i - m_j)^2} - \sqrt{\hat{s} - (m_i + m_j)^2} \right] \\
&\quad \cdot \sum_n \left(\frac{1}{\hat{u} - \tilde{m}_n^2} A_j^R(\tilde{q}_n) A_i^{L*}(\tilde{q}_n) \right) (1 - \cos \theta^*) , \\
F_{++--}^{ijBu} &= \frac{\sqrt{\hat{s}}}{4} \left[\sqrt{\hat{s} - (m_i - m_j)^2} + \sqrt{\hat{s} - (m_i + m_j)^2} \right] \\
&\quad \cdot \sum_n \left(\frac{1}{\hat{u} - \tilde{m}_n^2} A_j^R(\tilde{q}_n) A_i^{L*}(\tilde{q}_n) \right) (1 + \cos \theta^*) , \\
F_{+++-}^{ijBu} &= \frac{1}{4} \left[(m_i + m_j) \sqrt{\hat{s} - (m_i - m_j)^2} + (m_i - m_j) \sqrt{\hat{s} - (m_i + m_j)^2} \right] \\
&\quad \cdot \sum_n \left(\frac{1}{\hat{u} - \tilde{m}_n^2} A_j^R(\tilde{q}_n) A_i^{L*}(\tilde{q}_n) \right) \sin \theta^* . \tag{A.4}
\end{aligned}$$

The summation in (A.3, A.4) runs over the left and right squarks with the same flavor as the incoming quarks and mass \tilde{m}_n . The couplings in (A.1, A.3, A.4) have been defined in (12-17).

A.2 Leading log helicity amplitudes for $q\bar{q} \rightarrow \tilde{\chi}_i^0 \tilde{\chi}_j^0$.

In this subsection we include the one-loop leading log contributions to the seven basic amplitudes of (6). We use the various couplings defined in (12-17) and

$$\bar{m}_d \equiv \frac{m_d}{\cos \beta} , \quad \bar{m}_u \equiv \frac{m_u}{\sin \beta} , \tag{A.5}$$

$$Z_{di}^N \equiv Z_{3i}^N , \quad Z_{ui}^N \equiv Z_{4i}^N , \quad g = e/s_W , \quad g' = e/c_W , \tag{A.6}$$

$$\tilde{\beta}_0 = \frac{3}{4} C_A - \frac{n_g}{2} - \frac{n_h}{8} = -\frac{1}{4} , \quad \tilde{\beta}'_0 = -\frac{5}{6} n_g - \frac{n_h}{8} = -\frac{11}{4} , \tag{A.7}$$

while an \ln -symbol standing alone should be understood as

$$\ln \rightarrow \ln \frac{\hat{s}}{m_W^2} . \tag{A.8}$$

Denoting then by ($q = u, d$) the quark occurring in the initial state, and by ($q' = d, u$) the corresponding companion quark belonging to the same SU(2) doublet, and describing by M_S the effective average mass for the the squarks of the same flavor as the incoming quarks, the seven basic amplitudes of (6) are written as

$$\begin{aligned}
F_{-+--}^{ij}(\theta^*) &= F_{-+--}^{ijB}(\theta^*) \left[\frac{\alpha(1 + 26c_W^2)}{144\pi s_W^2 c_W^2} (2 \ln - \ln^2) - \frac{\alpha_s}{3\pi} \ln \frac{\hat{s}}{m_W^2} \right. \\
&\quad \left. - \frac{\alpha[\ln]}{8\pi s_W^2 m_W^2} \left(\frac{m_t^2}{\sin^2 \beta} + \frac{m_b^2}{\cos^2 \beta} \right) (\delta_{qt} + \delta_{qb}) \right] + F_{-+--}^{ijBs}(\theta^*) \left[\frac{\alpha(1 + 2c_W^2)}{16\pi s_W^2 c_W^2} (2 \ln - \ln^2) \right]
\end{aligned}$$

$$\begin{aligned}
& -\frac{3\alpha^2 g_{qL} \sqrt{\hat{s}} (1 + \cos \theta^*)}{16s_W^4 c_W^2 m_W^2 (\hat{s} - m_Z^2)} [\ln] \left\{ \sqrt{\hat{s} - (m_i - m_j)^2} \left[(Z_{4i}^{N*} Z_{4j}^N - Z_{4i}^N Z_{4j}^{N*}) \frac{m_t^2}{\sin^2 \beta} \right. \right. \\
& \left. \left. - (Z_{3i}^{N*} Z_{3j}^N - Z_{3i}^N Z_{3j}^{N*}) \frac{m_b^2}{\cos^2 \beta} \right] \right. \\
& \left. + \sqrt{\hat{s} - (m_i + m_j)^2} \left[(Z_{4i}^{N*} Z_{4j}^N + Z_{4i}^N Z_{4j}^{N*}) \frac{m_t^2}{\sin^2 \beta} - (Z_{3i}^{N*} Z_{3j}^N + Z_{3i}^N Z_{3j}^{N*}) \frac{m_b^2}{\cos^2 \beta} \right] \right\} \\
& + I_q^{(3)} \frac{\alpha^2 [\ln^2] \sqrt{\hat{s}}}{12s_W^4 c_W} \left\{ \frac{(1 + \cos \theta^*)}{\hat{t} - \tilde{m}^2(\tilde{q}_L)} \left[\sqrt{\hat{s} - (m_i - m_j)^2} - \sqrt{\hat{s} - (m_i + m_j)^2} \right] \right. \\
& \cdot [Z_{2j}^{N*} (Z_{1i}^N s_W + 6I_q^{(3)} Z_{2i}^N c_W) + Z_{2i}^N (Z_{1j}^{N*} s_W + 6I_q^{(3)} Z_{2j}^{N*} c_W)] \\
& - \frac{(1 + \cos \theta^*)}{\hat{u} - \tilde{m}^2(\tilde{q}_L)} \left[\sqrt{\hat{s} - (m_i - m_j)^2} + \sqrt{\hat{s} - (m_i + m_j)^2} \right] \\
& \cdot [Z_{2i}^{N*} (Z_{1j}^N s_W + 6I_q^{(3)} Z_{2j}^N c_W) + Z_{2j}^N (Z_{1i}^{N*} s_W + 6I_q^{(3)} Z_{2i}^{N*} c_W)] \left. \right\} \\
& - I_q^{(3)} \frac{\alpha^2 [\ln]}{\sqrt{\hat{s}} s_W^4} (1 + \cos \theta^*) \left\{ \left[\sqrt{\hat{s} - (m_i - m_j)^2} + \sqrt{\hat{s} - (m_i + m_j)^2} \right] \right. \\
& \cdot \left((2Z_{2i}^{N*} Z_{2j}^N + Z_{q'i}^{N*} Z_{q'j}^N) \left[\ln \frac{-\hat{t}}{\hat{s}} \right] - (2Z_{2i}^N Z_{2j}^{N*} + Z_{q'i}^N Z_{q'j}^{N*}) \left[\ln \frac{-\hat{u}}{\hat{s}} \right] \right) \\
& + \left[\sqrt{\hat{s} - (m_i - m_j)^2} - \sqrt{\hat{s} - (m_i + m_j)^2} \right] \\
& \cdot \left((2Z_{2i}^N Z_{2j}^{N*} + Z_{q'i}^N Z_{q'j}^{N*}) \left[\ln \frac{-\hat{t}}{\hat{s}} \right] - (2Z_{2i}^{N*} Z_{2j}^N + Z_{q'i}^{N*} Z_{q'j}^N) \left[\ln \frac{-\hat{u}}{\hat{s}} \right] \right) \left. \right\} \\
& + 2I_q^{(3)} \sqrt{\hat{s}} [\ln] \left\{ \frac{(1 + \cos \theta^*)}{\hat{t} - M_S^2} \left[\sqrt{\hat{s} - (m_i - m_j)^2} - \sqrt{\hat{s} - (m_i + m_j)^2} \right] \right. \\
& \cdot \left(\left[\ln \frac{-\hat{t}}{\hat{s}} \right] \left(\frac{\alpha^2}{12s_W^4 c_W} [Z_{2i}^N (Z_{1j}^{N*} s_W + 6I_q^{(3)} Z_{2j}^{N*} c_W) + Z_{2j}^{N*} (Z_{1i}^N s_W + 6I_q^{(3)} Z_{2i}^N c_W)] \right. \right. \\
& \left. \left. + \frac{\alpha^2 \tilde{m}_q^2}{4m_W^2 s_W^4} Z_{qj}^{N*} Z_{qi}^N \right) \right. \\
& \left. + \left[\ln \frac{-\hat{u}}{\hat{s}} \right] \left(\frac{\alpha^2}{12s_W^4 c_W} [Z_{2j}^{N*} (Z_{1i}^N s_W - 6I_q^{(3)} Z_{2i}^N c_W) + Z_{2i}^N (Z_{1j}^{N*} s_W - 6I_q^{(3)} Z_{2j}^{N*} c_W)] \right. \right. \\
& \left. \left. - \frac{\alpha^2 \tilde{m}_{q'}^2}{4m_W^2 s_W^4} Z_{q'i}^N Z_{q'j}^{N*} \right) \right) \\
& - \frac{(1 + \cos \theta^*)}{\hat{u} - M_S^2} \left[\sqrt{\hat{s} - (m_i - m_j)^2} + \sqrt{\hat{s} - (m_i + m_j)^2} \right] \\
& \left(\left[\ln \frac{-\hat{u}}{\hat{s}} \right] \left(\frac{\alpha^2}{12s_W^4 c_W} [Z_{2j}^N (Z_{1i}^{N*} s_W + 6I_q^{(3)} Z_{2i}^{N*} c_W) + Z_{2i}^{N*} (Z_{1j}^N s_W + 6I_q^{(3)} Z_{2j}^N c_W)] \right. \right. \\
& \left. \left. + \frac{\alpha^2 \tilde{m}_q^2}{4m_W^2 s_W^4} Z_{qi}^{N*} Z_{qj}^N \right) \right)
\end{aligned}$$

$$\begin{aligned}
& + \left[\ln \frac{-\hat{t}}{\hat{s}} \left(\frac{\alpha^2}{12s_W^4 c_W} [Z_{2i}^{N*} (Z_{1j}^N s_W - 6I_q^{(3)} Z_{2j}^N c_W) + Z_{2j}^N (Z_{1i}^{N*} s_W - 6I_q^{(3)} Z_{2i}^{N*} c_W)] \right. \right. \\
& \quad \left. \left. - \frac{\alpha^2 \bar{m}_{q'}^2}{4m_W^2 s_W^4} Z_{q'j}^N Z_{q'i}^{N*} \right) \right] \Big\} \\
& - \left[\frac{\tilde{\beta}_0}{s_W^4} + \frac{\tilde{\beta}'_0}{c_W^4} (1 - 2|Q_q|) \right] \frac{I_q^{(3)} \alpha^2 \sqrt{\hat{s}}}{(\hat{s} - m_Z^2)} (1 + \cos \theta^*) [(N^{ij} - N^{ij*}) \sqrt{\hat{s} - (m_i - m_j)^2} \\
& + (N^{ij} + N^{ij*}) \sqrt{\hat{s} - (m_i + m_j)^2}] [\ln] \quad , \tag{A.9}
\end{aligned}$$

$$\begin{aligned}
F_{-++++}^{ij}(\theta^*) & = F_{-++++}^{ijB}(\theta^*) \left[\frac{\alpha(1 + 26c_W^2)}{144\pi s_W^2 c_W^2} (2 \ln - \ln^2) - \frac{\alpha_s}{3\pi} \ln \frac{\hat{s}}{m_W^2} \right. \\
& - \frac{\alpha [\ln]}{8\pi s_W^2 m_W^2} \left(\frac{m_t^2}{\sin^2 \beta} + \frac{m_b^2}{\cos^2 \beta} \right) (\delta_{qt} + \delta_{qb}) \Big] + F_{-++++}^{ijBs}(\theta^*) \left[\frac{\alpha(1 + 2c_W^2)}{16\pi s_W^2 c_W^2} (2 \ln - \ln^2) \right] \\
& - \frac{3\alpha^2 g_{qL} \sin \theta^*}{16s_W^4 c_W^2 m_W^2 (\hat{s} - m_Z^2)} [\ln] \left\{ (m_i + m_j) \sqrt{\hat{s} - (m_i - m_j)^2} \left[(Z_{4i}^{N*} Z_{4j}^N - Z_{4i}^N Z_{4j}^{N*}) \frac{m_t^2}{\sin^2 \beta} \right. \right. \\
& - (Z_{3i}^{N*} Z_{3j}^N - Z_{3i}^N Z_{3j}^{N*}) \frac{m_b^2}{\cos^2 \beta} \Big] - (m_i - m_j) \sqrt{\hat{s} - (m_i + m_j)^2} \left[(Z_{4i}^{N*} Z_{4j}^N + Z_{4i}^N Z_{4j}^{N*}) \frac{m_t^2}{\sin^2 \beta} \right. \\
& \left. \left. - (Z_{3i}^{N*} Z_{3j}^N + Z_{3i}^N Z_{3j}^{N*}) \frac{m_b^2}{\cos^2 \beta} \right] \right\} \\
& + I_q^{(3)} \frac{\alpha^2 [\ln^2]}{12s_W^4 c_W} \left\{ \frac{\sin \theta^*}{\hat{t} - \tilde{m}^2(\tilde{q}_L)} [(m_i + m_j) \sqrt{\hat{s} - (m_i - m_j)^2} - (m_i - m_j) \sqrt{\hat{s} - (m_i + m_j)^2}] \right. \\
& \cdot [Z_{2j}^{N*} (Z_{1i}^N s_W + 6I_q^{(3)} Z_{2i}^N c_W) + Z_{2i}^N (Z_{1j}^{N*} s_W + 6I_q^{(3)} Z_{2j}^{N*} c_W)] \\
& - \frac{\sin \theta^*}{\hat{u} - \tilde{m}^2(\tilde{q}_L)} [(m_i + m_j) \sqrt{\hat{s} - (m_i - m_j)^2} + (m_i - m_j) \sqrt{\hat{s} - (m_i + m_j)^2}] \\
& \cdot [Z_{2i}^{N*} (Z_{1j}^N s_W + 3(2I_q^{(3)}) Z_{2j}^N c_W) + Z_{2j}^N (Z_{1i}^{N*} s_W + 3(2I_q^{(3)}) Z_{2i}^{N*} c_W)] \Big\} \\
& - I_q^{(3)} \frac{\alpha^2 [\ln]}{\hat{s} s_W^4} \sin \theta^* \left\{ [(m_i + m_j) \sqrt{\hat{s} - (m_i - m_j)^2} + (m_i - m_j) \sqrt{\hat{s} - (m_i + m_j)^2}] \right. \\
& \cdot \left((2Z_{2i}^{N*} Z_{2j}^N + Z_{q'i}^{N*} Z_{q'j}^N) \left[\ln \frac{-\hat{t}}{\hat{s}} \right] - (2Z_{2i}^{N*} Z_{2j}^N + Z_{q'i}^{N*} Z_{q'j}^N) \left[\ln \frac{-\hat{u}}{\hat{s}} \right] \right) \\
& + [(m_i + m_j) \sqrt{\hat{s} - (m_i - m_j)^2} - (m_i - m_j) \sqrt{\hat{s} - (m_i + m_j)^2}] \\
& \cdot \left((2Z_{2i}^N Z_{2j}^{N*} + Z_{q'i}^N Z_{q'j}^{N*}) \left[\ln \frac{-\hat{t}}{\hat{s}} \right] - (2Z_{2i}^N Z_{2j}^{N*} + Z_{q'i}^N Z_{q'j}^{N*}) \left[\ln \frac{-\hat{u}}{\hat{s}} \right] \right) \Big\} \\
& + I_q^{(3)} \frac{\alpha^2 [\ln]}{6s_W^4 c_W} \left\{ \frac{\sin \theta^*}{\hat{t} - M_S^2} [(m_i + m_j) \sqrt{\hat{s} - (m_i - m_j)^2} - (m_i - m_j) \sqrt{\hat{s} - (m_i + m_j)^2}] \right. \\
& \cdot \left(\left[\ln \frac{-\hat{t}}{\hat{s}} \right] [Z_{2i}^N (Z_{1j}^{N*} s_W + 6I_q^{(3)} Z_{2j}^{N*} c_W) + Z_{2j}^{N*} (Z_{1i}^N s_W + 6I_q^{(3)} Z_{2i}^N c_W)] + \frac{3\bar{m}_q^2 c_W}{m_W^2} Z_{qj}^N Z_{qi}^{N*} \right)
\end{aligned}$$

$$\begin{aligned}
& + \left[\ln \frac{-\hat{u}}{\hat{s}} \right] \left[Z_{2j}^{N*} (Z_{1i}^N s_W - 6I_q^{(3)} Z_{2i}^N c_W) + Z_{2i}^N (Z_{1j}^{N*} s_W - 6I_q^{(3)} Z_{2j}^{N*} c_W) - \frac{3\bar{m}_q^2 c_W}{m_W^2} Z_{q'i}^N Z_{q'j}^{N*} \right] \\
& - \frac{\sin \theta^*}{\hat{u} - M_S^2} [(m_i + m_j) \sqrt{\hat{s} - (m_i - m_j)^2} + (m_i - m_j) \sqrt{\hat{s} - (m_i + m_j)^2}] \\
& \cdot \left(\left[\ln \frac{-\hat{u}}{\hat{s}} \right] \left[Z_{2j}^N (Z_{1i}^{N*} s_W + 6I_q^{(3)} Z_{2i}^{N*} c_W) + Z_{2i}^{N*} (Z_{1j}^N s_W + 6I_q^{(3)} Z_{2j}^N c_W) + \frac{3\bar{m}_q^2 c_W}{m_W^2} Z_{qi}^{N*} Z_{qj}^N \right] \right. \\
& \left. + \left[\ln \frac{-\hat{t}}{\hat{s}} \right] \left[Z_{2i}^{N*} (Z_{1j}^N s_W - 6I_q^{(3)} Z_{2j}^N c_W) + Z_{2j}^N (Z_{1i}^{N*} s_W - 6I_q^{(3)} Z_{2i}^{N*} c_W) - \frac{3\bar{m}_q^2 c_W}{m_W^2} Z_{q'j}^N Z_{q'i}^{N*} \right] \right) \Big\} \\
& - \left[\frac{\tilde{\beta}_0}{s_W^4} + \frac{\tilde{\beta}'_0}{c_W^4} (1 - 2|Q_q|) \right] \frac{\alpha^2 I_q^{(3)}}{(\hat{s} - m_Z^2)} \sin \theta^* [(N^{ij} - N^{ij*})(m_i + m_j) \sqrt{\hat{s} - (m_i - m_j)^2} \\
& + (N^{ij} + N^{ij*})(m_i - m_j) \sqrt{\hat{s} - (m_i + m_j)^2}] [\ln] \quad , \tag{A.10}
\end{aligned}$$

$$\begin{aligned}
F_{++++}^{ij}(\theta^*) & = F_{++++}^{ijB}(\theta^*) \left[\frac{\alpha Q_q^2}{4\pi c_W^2} (2 \ln - \ln^2) - \frac{\alpha [\ln]}{4\pi s_W^2 m_W^2} \left(\frac{m_t^2}{\sin^2 \beta} \delta_{qt} + \frac{m_b^2}{\cos^2 \beta} \delta_{qb} \right) \right. \\
& - \left. \frac{\alpha_s}{3\pi} \ln \frac{\hat{s}}{m_W^2} \right] + F_{++++}^{ijBs}(\theta^*) \left[\frac{\alpha(1 + 2c_W^2)}{16\pi s_W^2 c_W^2} (2 \ln - \ln^2) \right] \\
& + \frac{3\alpha^2 g_{qR} \sin \theta^*}{16s_W^4 c_W^2 m_W^2 (\hat{s} - m_Z^2)} [\ln] \left\{ (m_i + m_j) \sqrt{\hat{s} - (m_i - m_j)^2} \left[(Z_{4i}^{N*} Z_{4j}^N - Z_{4i}^N Z_{4j}^{N*}) \frac{m_t^2}{\sin^2 \beta} \right. \right. \\
& - \left. \left. (Z_{3i}^{N*} Z_{3j}^N - Z_{3i}^N Z_{3j}^{N*}) \frac{m_b^2}{\cos^2 \beta} \right] \right. \\
& - \left. (m_i - m_j) \sqrt{\hat{s} - (m_i + m_j)^2} \left[(Z_{4i}^{N*} Z_{4j}^N + Z_{4i}^N Z_{4j}^{N*}) \frac{m_t^2}{\sin^2 \beta} - (Z_{3i}^{N*} Z_{3j}^N + Z_{3i}^N Z_{3j}^{N*}) \frac{m_b^2}{\cos^2 \beta} \right] \right\} \\
& + I_q^{(3)} \frac{\alpha^2 \bar{m}_q \bar{m}_{q'}}{4m_W^2 s_W^4} \sin \theta^* [\ln] \left\{ \frac{\ln \frac{-\hat{t}}{\hat{s}}}{\hat{t} - M_S^2} [(m_i + m_j) \sqrt{\hat{s} - (m_i - m_j)^2} \right. \\
& - \left. (m_i - m_j) \sqrt{\hat{s} - (m_i + m_j)^2}] (Z_{q'j}^N Z_{qi}^{N*} + Z_{q'i}^{N*} Z_{qj}^N) \right. \\
& - \left. \frac{\ln \frac{-\hat{u}}{\hat{s}}}{\hat{u} - M_S^2} [(m_i + m_j) \sqrt{\hat{s} - (m_i - m_j)^2} - (m_i - m_j) \sqrt{\hat{s} - (m_i + m_j)^2}] (Z_{q'i}^N Z_{qj}^{N*} + Z_{q'j}^N Z_{qi}^{N*}) \right\} \\
& - \frac{Q_q \tilde{\beta}'_0 \alpha^2 \sin \theta^*}{c_W^4 (\hat{s} - m_Z^2)} [(N^{ij} - N^{ij*})(m_i + m_j) \sqrt{\hat{s} - (m_i - m_j)^2} \\
& + (N^{ij} + N^{ij*})(m_i - m_j) \sqrt{\hat{s} - (m_i + m_j)^2}] [\ln] \quad , \tag{A.11}
\end{aligned}$$

$$\begin{aligned}
F_{+--+}^{ij}(\theta^*) & = F_{+--+}^{ijB}(\theta^*) \left[\frac{\alpha Q_q^2}{4\pi c_W^2} (2 \ln - \ln^2) - \frac{\alpha [\ln]}{4\pi s_W^2 m_W^2} \left(\frac{m_t^2}{\sin^2 \beta} \delta_{qt} + \frac{m_b^2}{\cos^2 \beta} \delta_{qb} \right) \right. \\
& - \left. \frac{\alpha_s}{3\pi} \ln \frac{\hat{s}}{m_W^2} \right] + F_{+--+}^{ijBs}(\theta^*) \left[\frac{\alpha(1 + 2c_W^2)}{16\pi s_W^2 c_W^2} (2 \ln - \ln^2) \right]
\end{aligned}$$

$$\begin{aligned}
& -\frac{3\alpha^2 g_{qR} \sqrt{\hat{s}} (1 + \cos \theta^*)}{16s_W^4 c_W^2 m_W^2 (\hat{s} - m_Z^2)} [\ln] \left\{ \sqrt{\hat{s} - (m_i - m_j)^2} \left[(Z_{4i}^{N*} Z_{4j}^N - Z_{4i}^N Z_{4j}^{N*}) \frac{m_t^2}{\sin^2 \beta} \right. \right. \\
& - \left. \left. (Z_{3i}^{N*} Z_{3j}^N - Z_{3i}^N Z_{3j}^{N*}) \frac{m_b^2}{\cos^2 \beta} \right] - \sqrt{\hat{s} - (m_i + m_j)^2} \left[(Z_{4i}^{N*} Z_{4j}^N + Z_{4i}^N Z_{4j}^{N*}) \frac{m_t^2}{\sin^2 \beta} \right. \right. \\
& - \left. \left. (Z_{3i}^{N*} Z_{3j}^N + Z_{3i}^N Z_{3j}^{N*}) \frac{m_b^2}{\cos^2 \beta} \right] \right\} \\
& - I_q^{(3)} \frac{\alpha^2 \sqrt{\hat{s}} \bar{m}_q \bar{m}_{q'}}{4m_W^2 s_W^4} \left\{ \frac{(1 + \cos \theta^*) \ln \frac{-\hat{t}}{\hat{s}}}{\hat{t} - M_S^2} \left[\sqrt{\hat{s} - (m_i - m_j)^2} - \sqrt{\hat{s} - (m_i + m_j)^2} \right] (Z_{q'j}^N Z_{qi}^{N*} + Z_{q'i}^{N*} Z_{qj}^N) \right. \\
& + \left. \frac{(1 + \cos \theta^*) \ln \frac{-\hat{u}}{\hat{s}}}{\hat{u} - M_S^2} \left[\sqrt{\hat{s} - (m_i - m_j)^2} + \sqrt{\hat{s} - (m_i + m_j)^2} \right] (Z_{q'i}^N Z_{qj}^{N*} + Z_{q'j}^N Z_{qi}^{N*}) \right\} \\
& + \frac{Q_q \tilde{\beta}'_0 \alpha^2 (1 + \cos \theta^*) \sqrt{\hat{s}}}{c_W^4 (\hat{s} - m_Z^2)} [(N^{ij} - N^{ij*}) (\sqrt{\hat{s} - (m_i - m_j)^2} \\
& - (N^{ij*} + N^{ij}) \sqrt{\hat{s} - (m_i + m_j)^2})] [\ln] \quad , \tag{A.12}
\end{aligned}$$

$$\begin{aligned}
F_{++++}^{ij}(\theta^*) &= F_{++++}^{ijB}(\theta^*) \left[\left(\frac{\alpha(1 + 26c_W^2)}{288\pi s_W^2 c_W^2} + \frac{\alpha}{72\pi c_W^2} \delta_{qd} + \frac{\alpha}{18\pi c_W^2} \delta_{qu} \right) (2 \ln - \ln^2) \right. \\
& - \left. \frac{\alpha_s}{3\pi} \ln \frac{\hat{s}}{m_W^2} - \frac{\alpha [\ln]}{8\pi s_W^2 m_W^2} \left(\frac{m_t^2}{\sin^2 \beta} \delta_{qt} + \frac{m_b^2}{\cos^2 \beta} \delta_{qb} \right) - \frac{\alpha [\ln]}{16\pi s_W^2 m_W^2} \left(\frac{m_t^2}{\sin^2 \beta} + \frac{m_b^2}{\cos^2 \beta} \right) (\delta_{qt} + \delta_{qb}) \right] \\
& + I_q^{(3)} \frac{\bar{m}_q \alpha^2 \sqrt{\hat{s}} [\ln^2]}{4m_W s_W^4} \left[\sqrt{\hat{s} - (m_i - m_j)^2} - \sqrt{\hat{s} - (m_i + m_j)^2} \right] \left[\frac{Z_{2j}^{N*} Z_{qi}^{N*} (1 + \cos \theta^*)}{\hat{t} - \tilde{m}^2(\tilde{q}_L)} \right. \\
& + \left. \frac{Z_{2i}^{N*} Z_{qj}^{N*} (1 - \cos \theta^*)}{\hat{u} - \tilde{m}^2(\tilde{q}_L)} \right] + I_q^{(3)} \frac{\alpha^2 \sqrt{\hat{s}} \bar{m}_q [\ln]}{12m_W s_W^4 c_W} \left[\sqrt{\hat{s} - (m_i - m_j)^2} - \sqrt{\hat{s} - (m_i + m_j)^2} \right] \\
& \cdot \left\{ \frac{(1 + \cos \theta^*)}{\hat{t} - M_S^2} \left[Z_{qi}^{N*} (Z_{1j}^{N*} s_W - 6I_q^{(3)} Z_{2j}^{N*} c_W) \ln \frac{-\hat{u}}{\hat{s}} \right. \right. \\
& + \left. \left. \left(6c_W (Z_{2j}^{N*} Z_{qi}^{N*} + Z_{2i}^N Z_{qj}^N) + 4s_W (Z_{1i}^{N*} Z_{qj}^{N*} + Z_{1j}^N Z_{qi}^N) \right) \ln \frac{-\hat{t}}{\hat{s}} \right] \right. \\
& + \left. \frac{(1 - \cos \theta^*)}{\hat{u} - M_S^2} \left[Z_{qj}^{N*} (Z_{1i}^{N*} s_W - 6I_q^{(3)} Z_{2i}^{N*} c_W) \ln \frac{-\hat{t}}{\hat{s}} \right. \right. \\
& + \left. \left. \left(6c_W (Z_{2i}^{N*} Z_{qj}^{N*} + Z_{2j}^N Z_{qi}^N) + 4s_W (Z_{1j}^{N*} Z_{qi}^{N*} + Z_{1i}^N Z_{qj}^N) \right) \ln \frac{-\hat{u}}{\hat{s}} \right] \right\} \quad , \tag{A.13}
\end{aligned}$$

$$\begin{aligned}
F_{+--+}^{ij}(\theta^*) &= F_{+--+}^{ijB}(\theta^*) \left[\left(\frac{\alpha(1 + 26c_W^2)}{288\pi s_W^2 c_W^2} + \frac{\alpha}{72\pi c_W^2} \delta_{qd} + \frac{\alpha}{18\pi c_W^2} \delta_{qu} \right) (2 \ln - \ln^2) \right. \\
& - \left. \frac{\alpha_s}{3\pi} \ln \frac{\hat{s}}{m_W^2} - \frac{\alpha [\ln]}{8\pi s_W^2 m_W^2} \left(\frac{m_t^2}{\sin^2 \beta} \delta_{qt} + \frac{m_b^2}{\cos^2 \beta} \delta_{qb} \right) - \frac{\alpha [\ln]}{16\pi s_W^2 m_W^2} \left(\frac{m_t^2}{\sin^2 \beta} + \frac{m_b^2}{\cos^2 \beta} \right) (\delta_{qt} + \delta_{qb}) \right] \\
& - I_q^{(3)} \frac{\bar{m}_q \alpha^2 \sqrt{\hat{s}} [\ln^2]}{4m_W s_W^4} \left[\sqrt{\hat{s} - (m_i - m_j)^2} + \sqrt{\hat{s} - (m_i + m_j)^2} \right] \left[\frac{Z_{2j}^{N*} Z_{qi}^{N*} (1 - \cos \theta^*)}{\hat{t} - \tilde{m}^2(\tilde{q}_L)} \right.
\end{aligned}$$

$$\begin{aligned}
& + \frac{Z_{2i}^{N*} Z_{qj}^{N*} (1 + \cos \theta^*)}{\hat{u} - \tilde{m}^2(\tilde{q}_L)} \Big] \\
& - I_q^{(3)} \frac{\alpha^2 \sqrt{\hat{s}} \tilde{m}_q [\ln]}{12 m_W s_W^4 c_W} \left[\sqrt{\hat{s} - (m_i - m_j)^2} + \sqrt{\hat{s} - (m_i + m_j)^2} \right] \\
& \cdot \left\{ \frac{(1 - \cos \theta^*)}{\hat{t} - M_S^2} \left[Z_{qi}^{N*} (Z_{1j}^{N*} s_W - 6 I_q^{(3)} Z_{2j}^{N*} c_W) \ln \frac{-\hat{u}}{\hat{s}} \right. \right. \\
& + \left(6 c_W (Z_{2j}^{N*} Z_{qi}^{N*} + Z_{2i}^N Z_{qj}^N) + 4 s_W (Z_{1i}^{N*} Z_{qj}^{N*} + Z_{1j}^N Z_{qi}^N) \right) \ln \frac{-\hat{t}}{\hat{s}} \Big] \\
& + \frac{(1 + \cos \theta^*)}{\hat{u} - M_S^2} \left[Z_{qj}^{N*} (Z_{1i}^{N*} s_W - 6 I_q^{(3)} Z_{2i}^{N*} c_W) \ln \frac{-\hat{t}}{\hat{s}} + \right. \\
& \left. \left. \left(6 c_W (Z_{2i}^{N*} Z_{qj}^{N*} + Z_{2j}^N Z_{qi}^N) + 4 s_W (Z_{1j}^{N*} Z_{qi}^{N*} + Z_{1i}^N Z_{qj}^N) \right) \ln \frac{-\hat{u}}{\hat{s}} \right] \right\} , \tag{A.14}
\end{aligned}$$

$$\begin{aligned}
F_{++++}^{ij}(\theta^*) &= F_{++++}^{ijB}(\theta^*) \left[\left(\frac{\alpha(1 + 26c_W^2)}{288\pi s_W^2 c_W^2} + \frac{\alpha}{72\pi c_W^2} \delta_{qd} + \frac{\alpha}{18\pi c_W^2} \delta_{qu} \right) (2 \ln - \ln^2) \right. \\
& - \frac{\alpha_s}{3\pi} \ln \frac{\hat{s}}{m_W^2} - \frac{\alpha [\ln]}{8\pi s_W^2 m_W^2} \left(\frac{m_t^2}{\sin^2 \beta} \delta_{qt} + \frac{m_b^2}{\cos^2 \beta} \delta_{qb} \right) - \frac{\alpha [\ln]}{16\pi s_W^2 m_W^2} \left(\frac{m_t^2}{\sin^2 \beta} + \frac{m_b^2}{\cos^2 \beta} \right) (\delta_{qt} + \delta_{qb}) \Big] \\
& + I_q^{(3)} \frac{\tilde{m}_q \alpha^2 [\ln^2] \sin \theta^*}{4 m_W s_W^4} [(m_i + m_j) \sqrt{\hat{s} - (m_i - m_j)^2} \\
& + (m_i - m_j) \sqrt{\hat{s} - (m_i + m_j)^2}] \left[\frac{Z_{2j}^{N*} Z_{qi}^{N*}}{\hat{t} - \tilde{m}^2(\tilde{q}_L)} - \frac{Z_{2i}^{N*} Z_{qj}^{N*}}{\hat{u} - \tilde{m}^2(\tilde{q}_L)} \right] \\
& + I_q^{(3)} \frac{\alpha^2 \tilde{m}_q [\ln] \sin \theta^*}{12 m_W s_W^4 c_W} [(m_i + m_j) \sqrt{\hat{s} - (m_i - m_j)^2} \\
& + (m_i - m_j) \sqrt{\hat{s} - (m_i + m_j)^2}] \left\{ \frac{1}{\hat{t} - M_S^2} \left[Z_{qi}^{N*} (Z_{1j}^{N*} s_W - 6 I_q^{(3)} Z_{2j}^{N*} c_W) \ln \frac{-\hat{u}}{\hat{s}} \right. \right. \\
& + \left(6 c_W (Z_{2j}^{N*} Z_{qi}^{N*} + Z_{2i}^N Z_{qj}^N) + 4 s_W (Z_{1i}^{N*} Z_{qj}^{N*} + Z_{1j}^N Z_{qi}^N) \right) \ln \frac{-\hat{t}}{\hat{s}} \Big] \\
& - \frac{1}{\hat{u} - M_S^2} \left[Z_{qj}^{N*} (Z_{1i}^{N*} s_W - 6 I_q^{(3)} Z_{2i}^{N*} c_W) \ln \frac{-\hat{t}}{\hat{s}} + \right. \\
& \left. \left. \left(6 c_W (Z_{2i}^{N*} Z_{qj}^{N*} + Z_{2j}^N Z_{qi}^N) + 4 s_W (Z_{1j}^{N*} Z_{qi}^{N*} + Z_{1i}^N Z_{qj}^N) \right) \ln \frac{-\hat{u}}{\hat{s}} \right] \right\} , \tag{A.15}
\end{aligned}$$

expressed in terms of the Born amplitudes $F_{\lambda_1 \lambda_2 \tau_i \tau_j}^{ijB}$ and its s-channel part $F_{\lambda_1 \lambda_2 \tau_i \tau_j}^{ijBs}$ appearing *e.g.* in (10, A.1-A.4).

Appendix B

B.1 Parton model kinematics for $\tilde{\chi}_i^0 \tilde{\chi}_j^0$ production.

The basic parton model expression for the hadron-hadron collision $A(q_1)B(q_2) \rightarrow \tilde{\chi}_i^0(p_i) + \tilde{\chi}_j^0(p_j) \dots$, is

$$d\sigma(AB \rightarrow \tilde{\chi}_i^0 \tilde{\chi}_j^0 \dots) = \sum_{q_1 q_2} \int \int dx_a dx_b f_{q_1/A}(x_a, Q) f_{q_2/B}(x_b, Q) d\hat{\sigma}(q_1 q_2 \rightarrow \tilde{\chi}_i^0 + \tilde{\chi}_j^0) \quad , \quad (\text{B.1})$$

with $\tilde{\chi}_i^0, \tilde{\chi}_j^0$ being the two produced massive particles of mass m_i, m_j . Here $f_{q_1/A}(x_a, Q)$ is the distribution function of partons of type $(q_1 = g, q, \bar{q})$, in the hadron of type A at a factorization scale Q .

Taking the AB -c.m. system as the lab-system, the lab-momenta of the produced $\tilde{\chi}_i^0$ and $\tilde{\chi}_j^0$ are

$$p_i^\mu = (E_i, p_T, p_i \cos \theta_i) \quad , \quad p_j^\mu = (E_j, -p_T, p_j \cos \theta_j) \quad , \quad (\text{B.2})$$

where their transverse momenta are obviously just opposite

$$p_T \equiv p_{Ti} = -p_{Tj} \quad , \quad (\text{B.3})$$

while their transverse energies $E_{Ti} = \sqrt{p_T^2 + m_i^2}$, $E_{Tj} = \sqrt{p_T^2 + m_j^2}$ are used to define

$$\begin{aligned} x_{Ti} &= \frac{2E_{Ti}}{\sqrt{s}} \quad , \quad \beta_{Ti} = p_T/E_{Ti} = \sqrt{1 - \frac{4m_i^2}{sx_{Ti}^2}} \quad , \\ x_{Tj} &= \frac{2E_{Tj}}{\sqrt{s}} \quad , \quad \beta_{Tj} = p_T/E_{Tj} = \sqrt{1 - \frac{4m_j^2}{sx_{Tj}^2}} \quad . \end{aligned} \quad (\text{B.4})$$

Note that

$$E_{Tj}^2 = E_{Ti}^2 + m_j^2 - m_i^2 \quad x_{Tj}^2 = x_{Ti}^2 + \frac{4(m_j^2 - m_i^2)}{s} \quad (\text{B.5})$$

The rapidities and production angles of $\tilde{\chi}_i^0, \tilde{\chi}_j^0$, in the lab-system, are related to their energies and momenta along the beam-axis of hadron A , (taken as the \hat{z} -axis) by

$$e^{2y_i} = \frac{E_i + p_i \cos \theta_i}{E_i - p_i \cos \theta_i} \quad , \quad e^{2y_j} = \frac{E_j + p_j \cos \theta_j}{E_j - p_j \cos \theta_j} \quad (\text{B.6})$$

The center-of-mass rapidity \bar{y} of the $\tilde{\chi}_i^0 \tilde{\chi}_j^0$ pair, and their respective rapidities y_i^* in their own c.m. frame, are defined as

$$y_i = \bar{y} + y_i^* \quad , \quad y_j = \bar{y} + y_j^* \quad , \quad (\text{B.7})$$

$$\Delta y \equiv y_i - y_j = y_i^* - y_j^* . \quad (\text{B.8})$$

The fractional momenta of the the incoming partons are expressed in terms of their lab-momenta by (compare (1, 31))

$$\begin{aligned} q_1 &= \frac{s}{2}(x_a, 0, 0, x_a) \quad , \quad q_2 = \frac{s}{2}(x_b, 0, 0, -x_b) \quad , \quad q = q_1 + q_2 \quad , \\ q^0 &= \frac{\sqrt{s}}{2}(x_a + x_b) = E_i + E_j \quad , \quad q^3 = \frac{\sqrt{s}}{2}(x_a - x_b) = (p_i \cos \theta_i + p_j \cos \theta_j) \quad , \end{aligned} \quad (\text{B.9})$$

which lead to

$$\begin{aligned} x_a &= \frac{1}{2}[x_{T_i} e^{y_i} + x_{T_j} e^{y_j}] = \frac{M}{\sqrt{s}} e^{\bar{y}} \quad , \\ x_b &= \frac{1}{2}[x_{T_i} e^{-y_i} + x_{T_j} e^{-y_j}] = \frac{M}{\sqrt{s}} e^{-\bar{y}} \quad , \end{aligned} \quad (\text{B.10})$$

$$\hat{s} \equiv M^2 = (q_1 + q_2)^2 = x_a x_b s = \frac{s}{4}[x_{T_i}^2 + x_{T_j}^2 + 2x_{T_i} x_{T_j} \cosh(\Delta y)] . \quad (\text{B.11})$$

Using this, \hat{s} , x_a , x_b may be calculated in terms of the final particle rapidities y_i , y_j and their transverse momenta. From them, \bar{y} is also obtained, and (y_i^*, y_j^*) through (B.7).

The remaining Mandelstam invariants of the subprocesses satisfy

$$\begin{aligned} \hat{t} &= (p_i - q_1)^2 = m_i^2 - M(E_i^* - p^* \cos \theta^*) = m_i^2 - \frac{x_{T_i}}{2} M \sqrt{s} e^{-y_i^*} = m_i^2 - \frac{s}{2} x_a x_{T_i} e^{-y_i} \\ &= m_j^2 - M(E_j^* - p^* \cos \theta^*) = m_j^2 - \frac{x_{T_j}}{2} M \sqrt{s} e^{y_j^*} = m_j^2 - \frac{s}{2} x_b x_{T_j} e^{y_j} \quad , \end{aligned} \quad (\text{B.12})$$

$$\begin{aligned} \hat{u} &= (p_j - q_1)^2 = m_i^2 - M(E_i^* + p^* \cos \theta^*) = m_i^2 - \frac{x_{T_i}}{2} M \sqrt{s} e^{y_i^*} = m_i^2 - \frac{s}{2} x_b x_{T_i} e^{y_i} \\ &= m_j^2 - M(E_j^* + p^* \cos \theta^*) = m_j^2 - \frac{x_{T_j}}{2} M \sqrt{s} e^{-y_j^*} = m_j^2 - \frac{s}{2} x_a x_{T_j} e^{-y_j} \quad , \end{aligned} \quad (\text{B.13})$$

$$\tau = \frac{\hat{s}}{s} = x_a x_b \quad , \quad (\text{B.14})$$

where θ^* describes $\tilde{\chi}_i^0$ production angle in the $\tilde{\chi}_i^0 \tilde{\chi}_j^0$ -c.m. frame (the $\tilde{\chi}_j^0$ one being $\pi - \theta^*$).

The energies of the two final particles in their c.m.-frame are

$$E_i^* = \frac{\hat{s} + m_i^2 - m_j^2}{2\sqrt{\hat{s}}} \quad , \quad E_j^* = \frac{\hat{s} + m_j^2 - m_i^2}{2\sqrt{\hat{s}}} \quad , \quad (\text{B.15})$$

their momentum is

$$p^* = \frac{1}{2M} [(M^2 - m_i^2 - m_j^2)^2 - 4m_i^2 m_j^2]^{\frac{1}{2}} \quad , \quad (\text{B.16})$$

and their velocities

$$\begin{aligned} \beta_i^* &= p^*/E_i^* = \frac{[(M^2 - m_i^2 - m_j^2)^2 - 4m_i^2 m_j^2]^{\frac{1}{2}}}{M^2 + (m_i^2 - m_j^2)} \quad , \\ \beta_j^* &= p^*/E_j^* = \frac{[(M^2 - m_i^2 - m_j^2)^2 - 4m_i^2 m_j^2]^{\frac{1}{2}}}{M^2 - (m_i^2 - m_j^2)} \quad . \end{aligned} \quad (\text{B.17})$$

We also have

$$\cos \theta^* = \frac{\tanh y_i^*}{\beta_i^*} = -\frac{\tanh y_j^*}{\beta_j^*} \quad , \quad \sin \theta^* = \frac{p_T}{p^*} \quad , \quad (\text{B.18})$$

$$\begin{aligned} \chi_i \equiv e^{2y_i^*} &= \frac{\hat{u} - m_i^2}{\hat{t} - m_i^2} = \frac{1 + \beta_i^* \cos \theta^*}{1 - \beta_i^* \cos \theta^*} \quad , \\ \chi_j \equiv e^{2y_j^*} &= \frac{\hat{t} - m_j^2}{\hat{u} - m_j^2} = \frac{1 - \beta_j^* \cos \theta^*}{1 + \beta_j^* \cos \theta^*} \quad , \end{aligned} \quad (\text{B.19})$$

Note that

$$\begin{aligned} \beta_i^* \cos \theta^* &= \frac{\hat{u} - \hat{t}}{\hat{u} + \hat{t}} = \frac{\chi_i - 1}{\chi_i + 1} \quad , \\ \chi_j &= \frac{\chi_i(m_j^2 - m_i^2) + M^2}{\chi_i M^2 + m_j^2 - m_i^2} \quad , \end{aligned} \quad (\text{B.20})$$

$$E_{Ti} = \frac{E_i^*}{\cosh y_i^*} \quad , \quad (\text{B.21})$$

$$p_T^2 = \frac{(M^2 + m_i^2 - m_j^2)^2 \chi_i - M^2 m_i^2 (1 + \chi_i)^2}{M^2 (1 + \chi_i)^2} \quad (\text{B.22})$$

$$x_{Ti}^2 = \frac{4(M^2 + m_i^2 - m_j^2)^2 \chi_i}{M^2 s (1 + \chi_i)^2} \quad x_{Tj}^2 = \frac{4(M^2 + m_j^2 - m_i^2)^2 \chi_j}{M^2 s (1 + \chi_j)^2} \quad (\text{B.23})$$

B.2 The basic distributions at LHC.

Using (B.1) we define

$$\frac{d\sigma}{dp_T^2 dy_i dy_j} = \tau S_{ij} \quad , \quad (\text{B.24})$$

or

$$\frac{d\sigma}{dM^2 d\chi_i d\bar{y}} = \frac{M^2 + m_i^2 - m_j^2}{M^2 (1 + \chi_i)^2} \tau S_{ij} \quad , \quad (\text{B.25})$$

or

$$\frac{d\sigma}{dM^2 d\bar{y} dp_T^2} = \frac{M}{2s \sqrt{p^{*2} - p_T^2}} S_{ij} \quad , \quad (\text{B.26})$$

where S_{ij} describes the contribution to (B.1) from all partons. Grouping together the gluon-gluon and $q\bar{q}$ parton contributions, we may write

$$S_{ij} \equiv S_{ij}^g + S_{ij}^{\text{quark}} \quad (\text{B.27})$$

with

$$S_{ij}^g \equiv g(x_a, Q)g(x_b, Q) \frac{d\hat{\sigma}(gg \rightarrow \tilde{\chi}_i^0 \tilde{\chi}_j^0)}{d\hat{t}}, \quad (\text{B.28})$$

$$S_{ij}^{\text{quark}} \equiv \sum_q \left[q(x_a, Q)\bar{q}(x_b, Q) \frac{d\hat{\sigma}(q\bar{q} \rightarrow \tilde{\chi}_i^0 \tilde{\chi}_j^0)}{d\hat{t}} + \bar{q}(x_a, Q)q(x_b, Q) \frac{d\hat{\sigma}(\bar{q}q \rightarrow \tilde{\chi}_i^0 \tilde{\chi}_j^0)}{d\hat{t}} \right], \quad (\text{B.29})$$

where $q = u, d, s, c, b$.

For the numerical calculations presented here, we use as an example the MRST2003c code for quark and gluon structure functions [11], taking the factorization scale as

$$Q = \frac{E_{T_i} + E_{T_j}}{4}. \quad (\text{B.30})$$

As seen from above, the basic quantities needed are $x_a, x_b, \hat{s} \equiv M^2, \hat{t}, \hat{u}$. In case of (B.24) these are calculated from (B.10, B.11, B.12, B.13). In case (B.25), Eqs.(B.19, B.7, B.15, B.16, B.17, B.18) must also be used.

Starting from this basic distribution, always assuming $m_i > m_j$, and imposing the cuts

$$|y_i| \leq Y_i, \quad |y_j| \leq Y_j \quad \text{with} \quad Y_i \leq Y_j, \quad (\text{B.31})$$

(in the numerical applications we take $Y_{i,j} = 2$) we get the single variable distributions defined in the following subsections.

B.2.1 The transverse energy and p_T distributions

$$\frac{d\sigma}{dx_{T_i}} = \int dy_i \int dy_j \frac{M^2 x_{T_i}}{2} S_{ij}, \quad \frac{d\sigma}{dp_{T_i}^2} = \int dy_i \int dy_j \frac{\hat{s}}{s} S_{ij}, \quad (\text{B.32})$$

where $\hat{s} = M^2$ is determined from (B.11), x_{T_j} from (B.5) and the integration limits are

$$\begin{aligned} y_{jmin} &= \max \left\{ \ln \left(\frac{x_{T_j}}{2 - x_{T_i} e^{-y_i}} \right); -Y_j \right\}, \\ y_{jmax} &= \min \left\{ \ln \left(\frac{2 - x_{T_i} e^{y_i}}{x_{T_j}} \right); Y_j \right\}, \end{aligned} \quad (\text{B.33})$$

$$\begin{aligned} y_{imax} &= -y_{imin} = \\ &= \min \left\{ Y_i; \cosh^{-1} \left(\frac{1}{x_{T_i}} \left(1 + \frac{m_i^2 - m_j^2}{s} \right) \right); \ln \left(\frac{2 - x_{T_j} e^{-Y_j}}{x_{T_i}} \right) \right\}. \end{aligned} \quad (\text{B.34})$$

The x_{T_i} range in (B.32) would be

$$\frac{2m_i}{\sqrt{s}} \leq x_{T_i} \leq 1 + \frac{m_i^2 - m_j^2}{s}, \quad (\text{B.35})$$

determined by the requirement that the middle constraint in (B.34) is meaningful.

B.2.2 The rapidity distribution

Since the y_i distribution has to be symmetric, we only consider the case of $y_i > 0$, for calculating the x_{T_i} -limits. Then in

$$\frac{d\sigma}{dy_i} = \int dx_{T_i} \int dy_j \frac{M^2 x_{T_i}}{2} S_{ij} , \quad (\text{B.36})$$

the y_j -limits are given by (B.33), while the limits for the x_{T_i} integration are

$$\begin{aligned} x_{T_{imin}} &= x_{T_{\min, \exp}} > \frac{2m_i}{\sqrt{s}} , \\ x_{T_{imax}} &= \min \left\{ \frac{1 + \frac{m_i^2 - m_j^2}{s}}{\cosh y_i} ; \frac{2e^{2Y_j \pm y_i} - \sqrt{\Delta_1}}{e^{2(Y_j \pm y_i)} - 1} ; 2e^{-y_i} \right\} \end{aligned} \quad (\text{B.37})$$

with

$$\Delta_1 = 4 \left[e^{2Y_j} + \frac{(m_i^2 - m_j^2)}{s} (1 - e^{2(Y_j \pm y_i)}) \right] , \quad (\text{B.38})$$

provided $\pm y_i \geq -Y_j$ and (of course) $y_i > 0$.

B.2.3 The invariant mass distribution

Using the c.m. rapidity \bar{y} defined above and (B.19), one obtains

$$\frac{d\sigma}{dM^2} = \int d\chi_i \int d\bar{y} \frac{(M^2 + m_i^2 - m_j^2)}{s(1 + \chi_i)^2} S_{ij} , \quad (\text{B.39})$$

where the integration limits are

$$\begin{aligned} \bar{y}_{max} &= \min \left\{ Y_i - \frac{1}{2} \ln \chi_i ; Y_j - \frac{1}{2} \ln \left(\frac{M^2 - \chi_i(m_i^2 - m_j^2)}{M^2 \chi_i - m_i^2 + m_j^2} \right) ; \ln \left(\frac{\sqrt{s}}{M} \right) \right\} , \\ \bar{y}_{min} &= \max \left\{ -Y_i - \frac{1}{2} \ln \chi_i ; -Y_j - \frac{1}{2} \ln \left(\frac{M^2 - \chi_i(m_i^2 - m_j^2)}{M^2 \chi_i - m_i^2 + m_j^2} \right) ; \right. \\ &\quad \left. - \ln \left(\frac{\sqrt{s}}{M} \right) \right\} , \end{aligned} \quad (\text{B.40})$$

$$\begin{aligned} \chi_{imax} &= \min \left\{ \frac{1 + \beta_i^*}{1 - \beta_i^*} ; \frac{M^2(s + (m_i^2 - m_j^2)e^{-2Y_j})}{M^4 e^{-2Y_j} + s(m_i^2 - m_j^2)} ; \right. \\ &\quad \left. \frac{(m_i^2 - m_j^2)(1 - e^{2(Y_i + Y_j)}) + \sqrt{\Delta_2}}{2M^2} ; \frac{s}{M^2} e^{2Y_i} \right\} , \\ \chi_{imin} &= \max \left\{ \frac{1 - \beta_i^*}{1 + \beta_i^*} ; \frac{M^4 e^{-2Y_j} + s(m_i^2 - m_j^2)}{M^2(s + (m_i^2 - m_j^2)e^{-2Y_j})} ; \right. \\ &\quad \left. \frac{2M^2}{(m_i^2 - m_j^2)(1 - e^{2(Y_i + Y_j)}) + \sqrt{\Delta_2}} ; \frac{M^2}{s} e^{-2Y_i} \right\} , \end{aligned} \quad (\text{B.41})$$

with

$$\Delta_2 = (m_i^2 - m_j^2)^2 (e^{2(Y_i+Y_j)} - 1)^2 + 4M^4 e^{2(Y_i+Y_j)} . \quad (\text{B.42})$$

B.2.4 The angular distribution

This is given by

$$\frac{d\sigma}{d\chi_i} = \int dM^2 \int d\bar{y} \frac{(M^2 + m_i^2 - m_j^2)}{s(1 + \chi_i)^2} S_{ij} , \quad (\text{B.43})$$

where the \bar{y} integration limits are as in (B.40), while for the M^2 integration we have the limits

$$\begin{aligned} M_{max}^2 &= \min \left\{ \chi_i s e^{2Y_i}; \frac{s}{\chi_i} e^{2Y_i}; M_+^2; M_+^{\prime 2}; s \right\} , \\ M_{min}^2 &= \max \left\{ L_1; L_2, L_3; M_-^2; M_-^{\prime 2} \right\} , \end{aligned} \quad (\text{B.44})$$

with

$$M_{\pm}^2 = \frac{1}{2} [\chi_i (m_i^2 - m_j^2 + s e^{2Y_j}) \pm \sqrt{\Delta_3}] , \quad (\text{B.45})$$

$$\Delta_3 = \chi_i^2 (m_i^2 - m_j^2 + s e^{2Y_j})^2 - 4s (m_i^2 - m_j^2) e^{2Y_j} , \quad (\text{B.46})$$

$$M_{\pm}^{\prime 2} = \frac{1}{2\chi_i} [m_i^2 - m_j^2 + s e^{2Y_j} \pm \sqrt{\Delta_3'}] , \quad (\text{B.47})$$

$$\Delta_3' = (m_i^2 - m_j^2 + s e^{2Y_j})^2 - 4s (m_i^2 - m_j^2) \chi_i^2 e^{2Y_j} , \quad (\text{B.48})$$

$$L_1 = \frac{\chi_i (m_i^2 - m_j^2) (e^{2(Y_j+Y_i)} - 1)}{\chi_i^2 e^{2(Y_j+Y_i)} - 1} , \quad (\text{B.49})$$

$$L_2 = \frac{\chi_i (m_i^2 - m_j^2) (e^{2(Y_j+Y_i)} - 1)}{e^{2(Y_j+Y_i)} - \chi_i^2} , \quad (\text{B.50})$$

$$L_3 = \frac{1}{2} \left[\frac{4m_i^2}{1 - \chi^2} - 2(m_i^2 - m_j^2) + \sqrt{\Delta_4} \right] , \quad (\text{B.51})$$

$$\chi = \frac{\chi_i - 1}{\chi_i + 1} , \quad (\text{B.52})$$

$$\Delta_4 = 16 \left[\frac{m_i^4}{(1 - \chi^2)^2} - \frac{m_i^2 (m_i^2 - m_j^2)}{1 - \chi^2} \right] . \quad (\text{B.53})$$

References

- [1] see e.g. D.P. Roy, *Acta Phys. Polon.* **B34**:3417 (2003) , hep-ph/0303106; F.E. Paige, hep-ph/0307342, hep-ph/0211017.
- [2] B.C. Allanach, G.A. Blair, S. Kraml, H.U. Martyn, G. Polesello, W. Porod and P.M. Zerwas, hep-ph/0403133; K. Desch, J. Kalinowski, G. Moortgat-Pick, M.M. Nojiri and G. Polesello, hep-ph/0312069; G. Weiglein, hep-ph/0404108.
- [3] A.H. Chamseddine, R. Arnowitt and P. Nath, *Phys. Rev. Lett.* **49**:970 (1982); R. Barbieri, S. Ferrara and C.A. Savoy, *Phys. Lett.* **B119**:343 (1982); L. Hall, J. Lykken and S. Weinberg *Phys. Rev.* **D27**:2359 (1983); L. Randall and R. Sundrum, *Nucl. Phys.* **B557**:79 (1999); G. Giudice, M. Luty, H. Murayama and R. Rattazzi, *JHEP* **9812**:027 (1998); J.A. Bagger, T. Moroi and E. Poppitz, *JHEP* **0004**:009 (2000).
- [4] M. Drees, *Pramana* **51**:87(1998); M.S. Turner, J.A. Tyson, astro-ph/9901113, *Rev. Mod. Phys.* **71S**:145(1999); M.M. Nojiri, hep-ph/0305192; M. Drees hep-ph/0210142; J. Ellis, astro-ph/0304183; D.N. Spergel *et.al.* arXiv:astro-ph/0302209; G. Jungman, M. Kamionkowski and K. Griest, *Phys. Rep.* **267**:195 (1996); M. Kamionkowski, hep-ph/0210370; L. Roszkowski, hep-ph/0404052.
- [5] D.S.Akerib, S.M. Carrol, M. Kamionkowski and S. Ritz, hep-ph/0201178.
- [6] G.J. Gounaris, J. Layssac, P.I. Porfyriadis, F.M. Renard, arXiv:hep-ph/0309032, to appear in *Phys.Rev.D*.
- [7] G.J. Gounaris, J. Layssac, P.I. Porfyriadis, F.M. Renard, arXiv:hep-ph/0311076, *EPJ* **C32**:561(2004).
- [8] B.C. Allanach et al, *Eur. Phys. J.* **C25**:113 (2002), hep-ph/0202233; G. Weiglein, hep-ph/0301111.
- [9] R. Arnowitt and B. Dutta, talk at 10th Int. Conf. on Supersymmetry and Unification of Fundamental Interactions (SUSY02), Hamburg, 2002 (hep-ph/0211042).
- [10] C.H. Chen, M. Drees and J.F. Gunion, *Phys. Rev.* **D55**:330 (1997) and (E) *Phys. Rev.* **D60**:039901 (1999); J. Amundson *et.al.* , Report of the Snowmass Sypersymmetry Theory Working Group, hep-ph/9609374; A. Djouadi, Y. Mambrini and M. Mühlleitner, hep-ph/0104115, *Eur. Phys. J.* **C20**:563 (2001).
- [11] MRST2003c.f can be obtained from <http://durpdg.dur.ac.uk/hepdata/pdf.html>. See also A.D. Martin, R.G. Roberts, W.J. Stirling and R.S. Thorne, hep-ph/0307263; R.S. Thorne, hep-ph/0309343.
- [12] S. Dawson , E. Eichten and C. Quigg, *Phys. Rev.* **D31**:1581 (1985).
- [13] H. Baer, K. Hagiwara and X. Tata, *Phys. Rev.* **D35**:1598 (1987)

- [14] M. Beccaria, M. Melles, F.M. Renard, S. Trimarchi and C. Verzegnassi, arXiv:hep-ph/0304110, IJMP **A18**:5069 (2003).
- [15] A. Denner and S. Pozzorini Eur. Phys. J. **C18**:461 (2001); *ibid* Eur. Phys. J. **C21**:63 (2001).
- [16] M. Beccaria, F.M. Renard and C. Verzegnassi, hep-ph/0402028, to appear in Phys. Rev. D.
- [17] W. Beenakker, M. Klasen, M Krämer .Plehn, M. Spira and P.M. Zerwas, Phys. Rev. Lett. **83**:3780 (1999).
- [18] PLATON codes can be downloaded from <http://dtp.physics.auth.gr/platon/>
- [19] M. Jacob and G.C. Wick, Annals of Phys. **7**:404 (1959).
- [20] H.Liang, Ma Wen-Gan, Jiang Yi, Zhou Mian-Lai and Zhou Hong, Commun. Theor. Phys. **34**:115 (2000).
- [21] see *e.g.* G.J. Gounaris, C. Le Mouël and P.I. Porfyriadis Phys. Rev. **D65**:035002 (2002); G.J. Gounaris and C. Le Mouël Phys. Rev. **D66**:055007 (2002).
- [22] J. Rosiek, Phys. Rev. **D41**:3464 (1990), hep-ph/9511250(E).
- [23] H. Baer, R. Munroe, X. Tata, Phys. Rev. **D54**:6735 (1996); H. Baer, A. Bartl, D. Karatas, W. Majerotto, X. Tata Int. J. Mod. Phys. **A4**:4111 (1989).

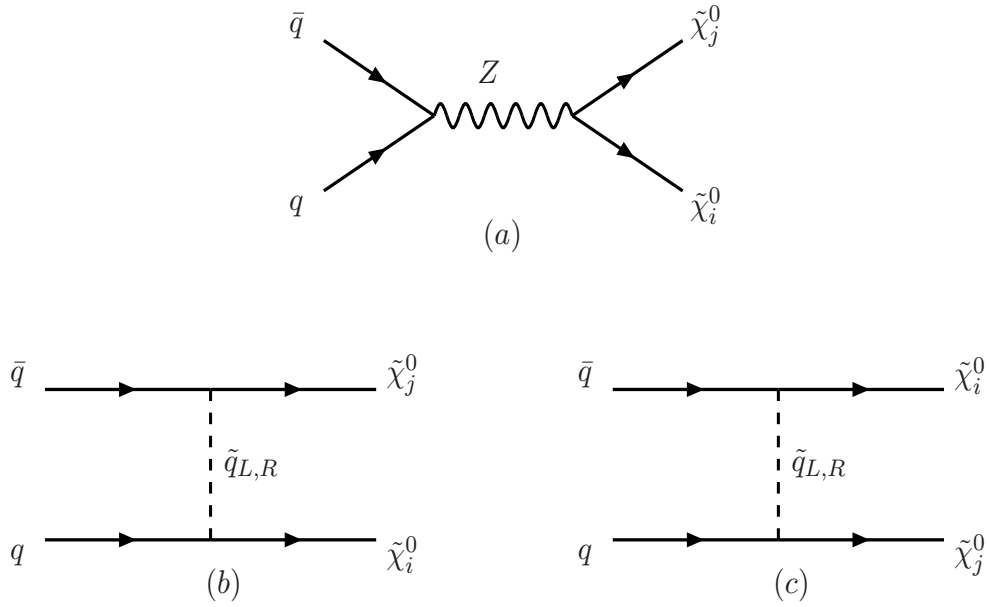


Figure 1: Feynman diagrams for $q\bar{q} \rightarrow \tilde{\chi}_i^0 \tilde{\chi}_j^0$.

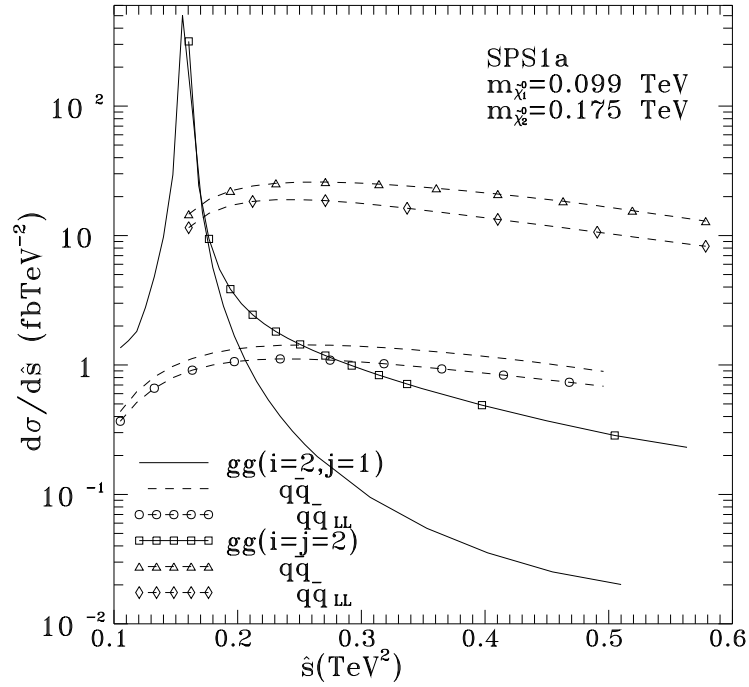


Figure 2: The \hat{s} distributions in the SPS1a model of [8].

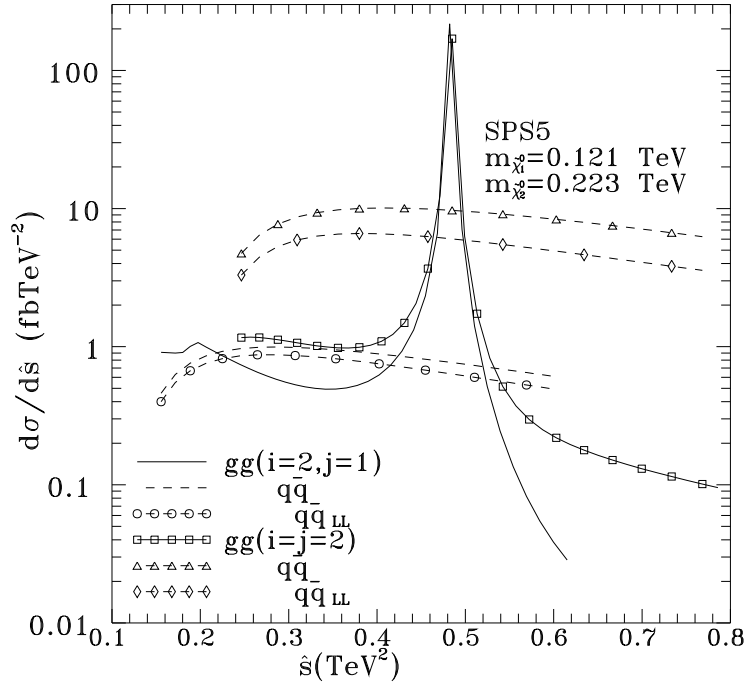


Figure 3: The \hat{s} distributions in the SPS5 model of [8].

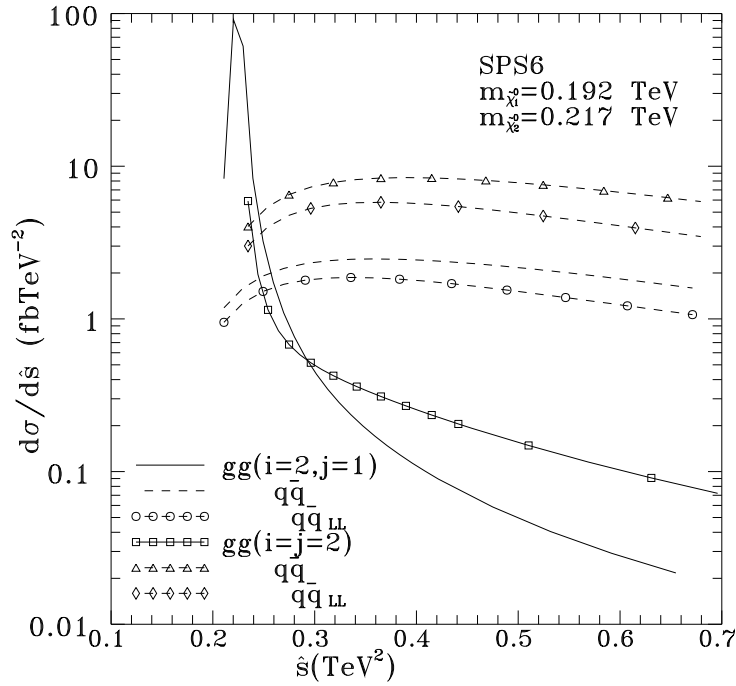


Figure 4: The \hat{s} distributions in the SPS6 model of [8].

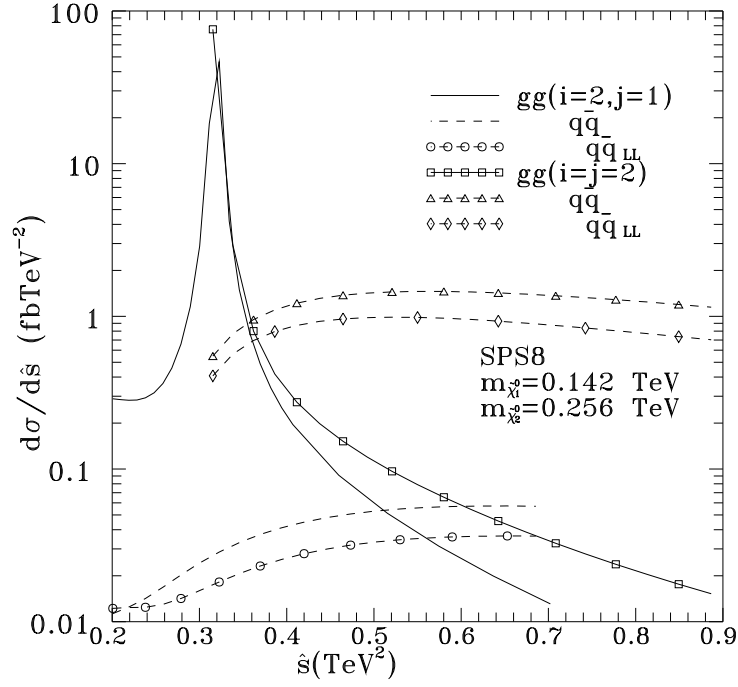


Figure 5: The \hat{s} distributions in the SPS8 model of [8].

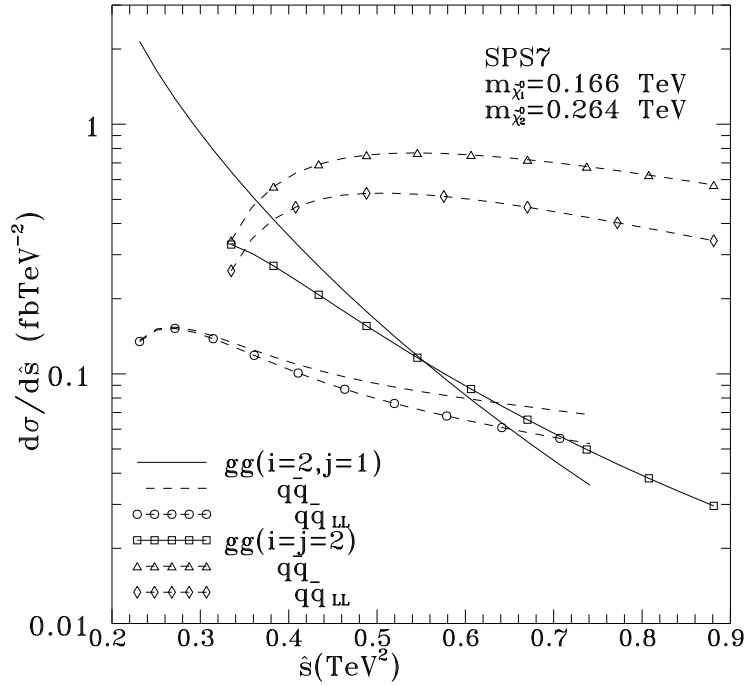


Figure 6: The \hat{s} distributions in the SPS7 model of [8].

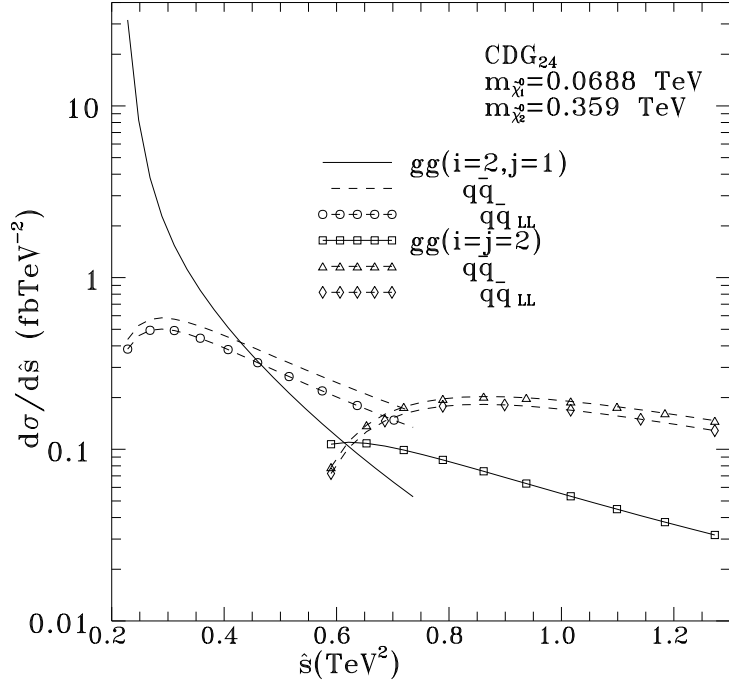


Figure 7: The \hat{s} distributions in the CDG_{24} model of [10].

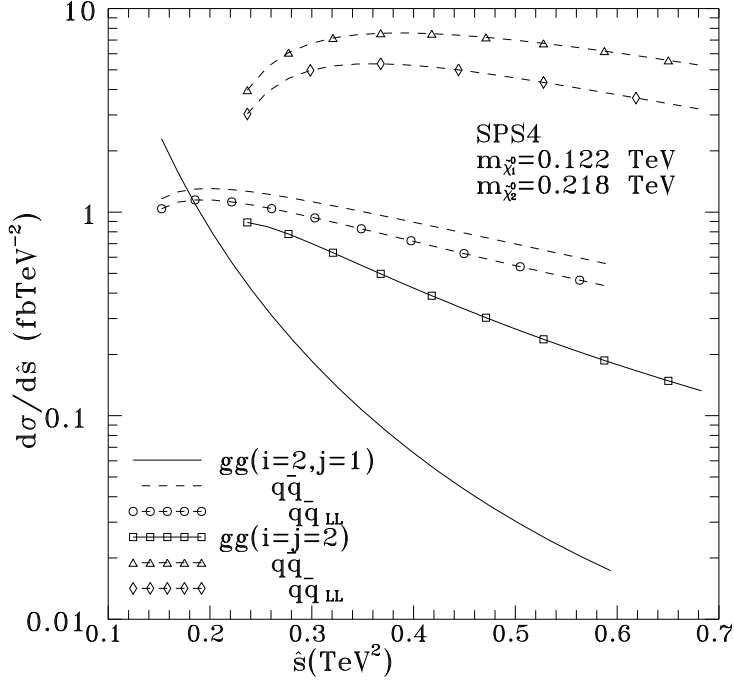


Figure 8: The \hat{s} distributions in the SPS4 model of [8].

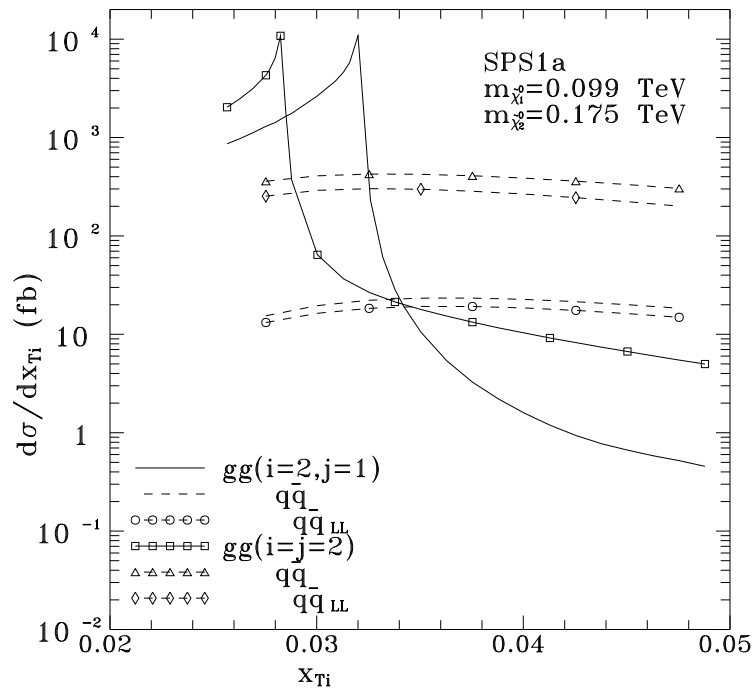


Figure 9: The x_{Ti} distribution in SPS1a of [8].

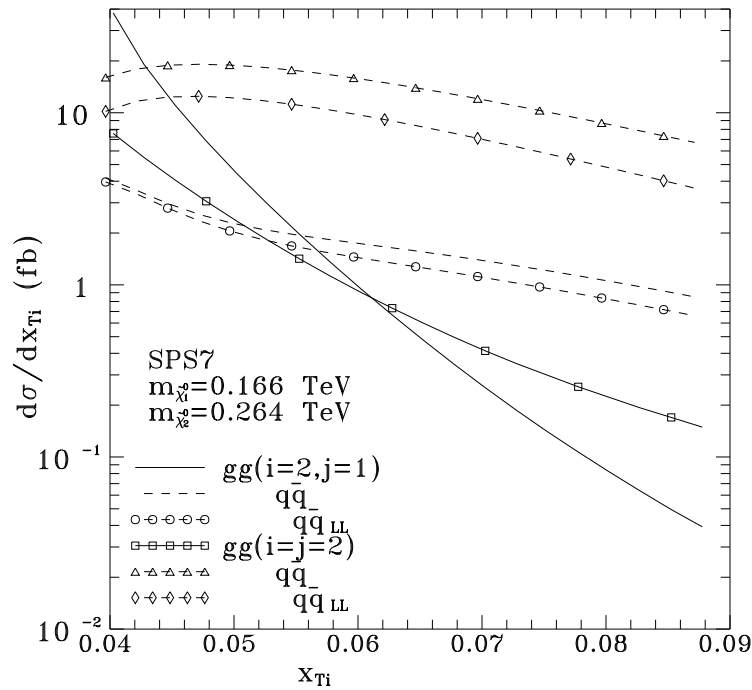


Figure 10: The x_{Ti} distribution in SPS7 of [8].

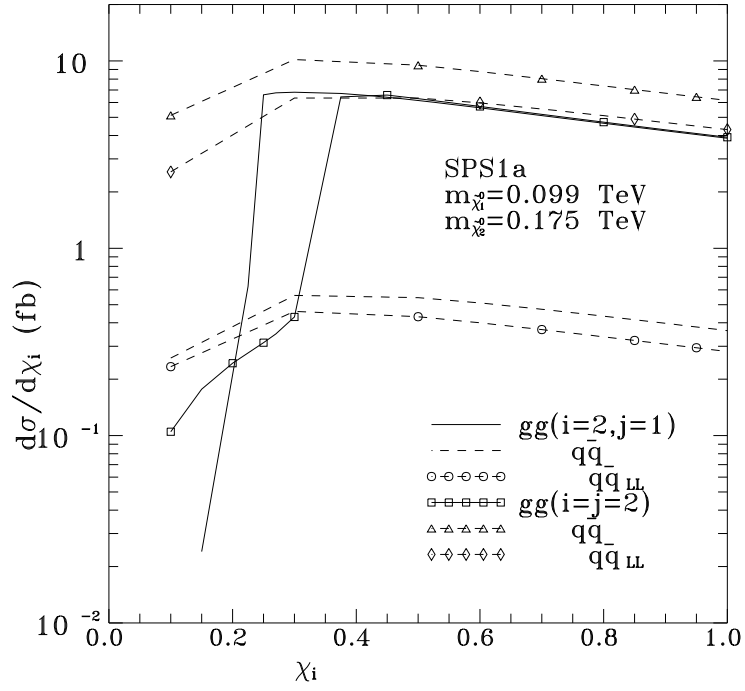


Figure 11: The χ_i distribution in SPS1a of [8].

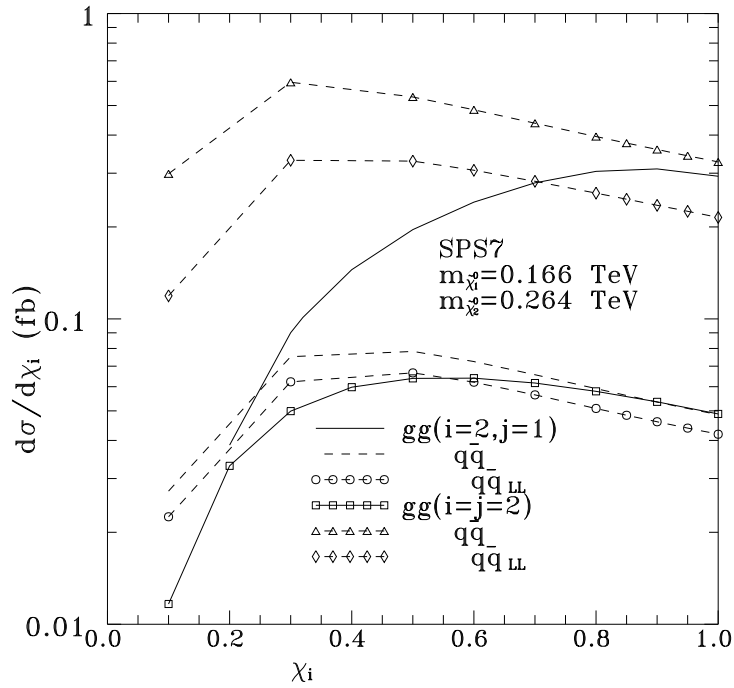


Figure 12: The χ_i distribution in SPS7 of [8].